Published online 18 May 2020 *Nucleic Acids Research, 2020, Vol. 48, No. 11* ***5891–5906***
doi: 10.1093/nar/gkaa344

Che-1/AATF binds to RNA polymerase I machinery and sustains ribosomal RNA gene transcription

Cristina Sorino[1,2,†], Valeria Catena[1,†], Tiziana Bruno[1], Francesca De Nicola[1], Stefano Scalera[1], Gianluca Bossi[3], Francesca Fabretti[4,5], Miguel Mano[6], Enrico De Smaele[2], Maurizio Fanciulli[1,*] and Simona Iezzi[1,*]

[1]SAFU Laboratory, Department of Research, Advanced Diagnostics and Technological Innovation, Translational Research Area, IRCCS Regina Elena National Cancer Institute, 00144 Rome, Italy, [2]Department of Experimental Medicine, Sapienza–University of Rome, 00161 Rome, Italy, [3]Oncogenomic and Epigenetic Unit, Department of Research, Advanced Diagnostics and Technological Innovation, Translational Research Area, IRCCS Regina Elena National Cancer Institute, 00144 Rome, Italy, [4]Department II of Internal Medicine and Center for Molecular Medicine Cologne, University of Cologne, Faculty of Medicine and University Hospital of Cologne, 50937 Cologne, Germany, [5]CECAD, University of Cologne, Faculty of Medicine and University Hospital of Cologne, 50931 Cologne, Germany and [6]Center for Neuroscience and Cell Biology (CNC), University of Coimbra, Coimbra 3060 197, Portugal

Received July 24, 2019; Revised April 21, 2020; Editorial Decision April 22, 2020; Accepted April 24, 2020

ABSTRACT

Originally identified as an RNA polymerase II interactor, Che-1/AATF (Che-1) has now been recognized as a multifunctional protein involved in cell-cycle regulation and cancer progression, as well as apoptosis inhibition and response to stress. This protein displays a peculiar nucleolar localization and it has recently been implicated in pre-rRNA processing and ribosome biogenesis. Here, we report the identification of a novel function of Che-1 in the regulation of ribosomal RNA (rRNA) synthesis, in both cancer and normal cells. We demonstrate that Che-1 interacts with RNA polymerase I and nucleolar upstream binding factor (UBF) and promotes RNA polymerase I-dependent transcription. Furthermore, this protein binds to the rRNA gene (rDNA) promoter and modulates its epigenetic state by contrasting the recruitment of HDAC1. Che-1 downregulation affects RNA polymerase I and UBF recruitment on rDNA and leads to reducing rDNA promoter activity and 47S pre-rRNA production. Interestingly, Che-1 depletion induces abnormal nucleolar morphology associated with re-distribution of nucleolar proteins. Finally, we show that upon DNA damage Che-1 re-localizes from rDNA to *TP53* gene promoter to induce cell-cycle arrest. This previously uncharacterized function of Che-1 confirms the important role of this protein in the regulation of ribosome biogenesis, cellular proliferation and response to stress.

INTRODUCTION

Ribosome biogenesis is a highly regulated multistep process that controls cell growth and proliferation. Due to this fundamental role in cellular homeostasis, it is not surprising that defects in every step of this process have been associated with the development of many diseases, including cancer (1). The first and key regulatory step of ribosome biogenesis is represented by the transcription of ribosomal RNA (rRNA) genes by RNA polymerase (pol) I in the nucleolus (1,2). Human cells contain hundreds of rRNA genes arranged in arrays of tandem repeats distributed amongst the five acrocentric chromosomes (2). Each repeat is transcribed as a 47S pre-rRNA precursor, which is subsequently chemically modified and processed to form the mature 5.8S, 18S and 28S rRNAs, which will be assembled into ribosomes. Notably, not all repeats are transcriptionally active but almost 50% of them are kept transcriptionally silent, mainly by epigenetic mechanisms (3). Activity of RNA pol I is tightly regulated by interactions with many auxiliary factors that mediate promoter recognition and contribute to transcription initiation, elongation and termination (4,5). The upstream binding factor (UBF) is one of the main regulators of ribosomal RNA gene (rDNA) transcription, as it is involved in multiple steps of this process, such as pre-initiation complex assembly, promoter escape (6) and elongation (7). Moreover, it binds throughout the entire length

*To whom correspondence should be addressed. Tel: +39 06 5266 2578; Fax: +39 06 5266 2980; Email: simona.iezzi@ifo.gov.it
Correspondence may also be addressed Maurizio Fanciulli. Tel: +39 06 5266 2800; Fax: +39 06 5266 2980; Email: maurizio.fanciulli@ifo.gov.it
†The authors wish it to be known that, in their opinion, the first two authors should be regarded as joint First Authors.

of the rRNA gene and it plays a critical role in establishing and maintaining the euchromatic state of active rDNA repeats (8). As many key components of the RNA pol I transcriptional machinery, its activities are finely regulated by multiple interacting partners and post-translational modifications, such as acetylation and phosphorylation (9–11).

Che-1/AATF (Che-1) is an evolutionary conserved protein originally identified as an RNA pol II-interacting factor (12). Studies conducted over the last 20 years have linked Che-1 to many cellular processes, such as transcriptional regulation, cell-cycle and apoptosis control, cellular response to DNA damage and stress, and cancer progression (13–17). Multiple post-translational modifications, namely phosphorylation, ubiquitination, poly-ADP-ribosylation and acetylation, modulate Che-1 activities in response to different stimuli (13,18). Amongst these modifications, phosphorylation by checkpoint kinases ataxia telangiectasia mutated (ATM) and Chk2 plays a crucial role in regulating Che-1 activity in response to genotoxic and cellular stress. Indeed, this modification completely modifies Che-1 activity shifting this protein from the regulation of pathways involved in cell-cycle progression to ones involved in cell-cycle arrest and survival. Specifically, phosphorylated Che-1 binds to *TP53* gene promoter, through its interaction with NF-κB subunit p65, thus promoting its transcription and contributing to the increase of p53 protein levels associated with the cellular response to stress (19). Moreover, it directly binds to p53 and specifically directs this protein towards the transcription of genes involved in cell-cycle arrest over those that induce apoptosis (20). Even if a cytoplasmic localization of Che-1 has been reported (21–23), this protein mainly localizes to the nucleoli. Interestingly, it has also been demonstrated that UV damage induces Che-1 translocation from the nucleolus to the nucleoplasm, where it interacts with c-Jun and participates in c-Jun-mediated apoptosis (24). In line with its nucleolar localization, over the last few years, a pivotal role for Che-1 in ribosome biogenesis is emerging. Indeed, two independent RNAi screenings have identified this protein as a factor involved in ribosome subunit production (25,26). Moreover, it has recently been shown that Che-1 forms a complex, named ANN complex, with nucleolar factors neuroguidin (NGDN) and NOL10; this complex is involved in the early steps of pre-rRNA processing, thus contributing to the nucleolar steps of 40S subunit biosynthesis (27). In agreement with these results, a reduced number of ribosomes has been detected by electron microscopy in mouse embryos mutant for *Traube* (Che-1 mouse orthologue) (28). However, the role of Che-1 in ribosome biogenesis is yet to be fully clarified.

In this study, we highlight a new role for Che-1 in RNA pol I-dependent transcription. We demonstrate that Che-1 promotes rRNA synthesis by binding to rDNA loci and interacting with RNA pol I machinery. Upon DNA damage, Che-1 re-localizes from rDNA to DNA damage gene promoters thus halting rRNA synthesis and promoting cell-cycle arrest. These results support the pivotal role of Che-1 in ribosome biogenesis and confirm this protein as a key factor in the regulation of cellular homeostasis.

MATERIALS AND METHODS

Cell lines, transfections and reagents

Human HCT116, 293T and HeLa cell lines were cultured in Dulbecco's Modified Eagle Medium (DMEM, Euroclone) supplemented with 10% inactivated foetal bovine serum (FBS, Thermo Fisher Scientific), 2 mM glutamine (Thermo Fisher Scientific) and 40 μg/ml gentamicin. BJ human fibroblasts were maintained in Minimum Essential Medium (MEM, Euroclone) supplemented with 10% inactivated FBS (Thermo Fisher Scientific), 1 mM sodium pyruvate (Euroclone), 10 mM non-essential amino acids (Euroclone), 2 mM glutamine and 40 μg/ml gentamicin. shChe-1 HCT116 inducible cell line was generated as described by Bruno *et al*. (29). All cell lines were cultured at 37°C, in a humidified atmosphere with 5% CO_2. Mycoplasma contamination was periodically checked by polymerase chain reaction (PCR) analysis, using the following primers:

Forward: 5′ - ACTCCTACGGGAGGCAGCAGTA - 3′
Reverse: 5′ - TCGACCATCTGTCACTCTGTTAAC - 3′

Transfection experiments were carried out using calcium phosphate precipitation or Lipofectamine 3000 Transfection System (Thermo Fisher Scientific) according to the manufacturer's instructions. Cells were analysed 48–72 h after transfection by western blot (WB), real-time PCR or immunofluorescence. Che-1 (Che-1 myc, Che-1^{S187A} myc, Che-1 myc deletion mutants) and HDAC1 myc expressing vectors have already been described (12,19,30–31). Stealth siRNA oligonucleotides targeting Che-1 (siChe-1, cat. n. 1299003–HSS120158 and siChe-1 b, cat. n. 1299003–HSS120159) or a control sequence (siControl, cat. n. 12935300), and RNAse A were purchased from Thermo Fisher Scientific. CX-5461 and LY2603618 were purchased from SelleckChem, whereas actinomycin D, caffeine and Adriamycin (Adr) were obtained from Sigma-Aldrich. The UVB irradiation was performed using a Bio-Sun irradiation apparatus (Vilbert Lourmat, Marne-la-Vallèe, France) following the manufacturer's instructions.

Immunofluorescence

Cells grown on coverslips were fixed in 4% formaldehyde for 10 min and then permeabilized with 0.1% Triton X-100 in phosphate-buffered saline (PBS) for 5 min at room temperature. Cells were subsequently stained for 2 h with primary antibodies, after which they were rinsed three-times with PBS and stained for 45 min with Alexa-Fluor-594- and Alexa-Fluor-488-conjugated anti-rabbit or anti-mouse secondary antibodies (Thermo Fisher Scientific). Nuclei were visualized by staining with 1 μg/ml Hoechst dye 33258 (Sigma-Aldrich). Nucleoli were detected with SYTO RNAselect Green Fluorescent Cell Stain (Thermo Fisher Scientific). For 5-fluorouridine (5-FUrd) incorporation assay, cells were incubated with 5 mM 5-FUrd (Sigma-Aldrich) for 10 min before the analysis. Cells were fixed in 2% formaldehyde for 10 min and then permeabilized with 0.5% Triton X-100 in PBS for 5 min at room temperature. Cells were then blocked in 3% bovine serum albumin (BSA) in PBS for 1 h and stained with anti-BrdU antibody (Sigma-Aldrich). Images were acquired using a fluorescence mi-

croscope with a 60× objective (Zeiss, Germany) and processed with AxioVision Software. Pearson's correlation coefficient was calculated using ImageJ software with Coloc2 analysis.

Proximity ligation assay

Cells grown on coverslips were fixed in 4% formaldehyde for 10 min and then permeabilized with 0.1% Triton X-100 in PBS for 5 min at room temperature. *In situ* proximity ligation assay (PLA) was performed using the Duolink *In Situ* Reagents (Sigma-Aldrich) according to the manufacturer's instructions.

Cellular extracts and immunoprecipitation

For the nuclear extract preparation cells were incubated in ice for 5 min in hypotonic buffer (50 mM TRIS pH 7.5, 10 mM NaCl, 5 mM ethylenediaminetetraacetic acid (EDTA), 0.05% NP40) supplemented with protease and phosphatase inhibitors (1 μg/ml aprotinin, 1 μg/ml leupeptin, 1 mM Na_3VO_4, 10 mM phenylmethylsulfonyl fluoride (PMSF)). Nuclei were isolated by low-speed centrifugation, re-suspended in buffer C (20 mM HEPES pH 7.9, 25% glycerol, 420 mM NaCl, 1.5 mM $MgCl_2$, 0.2 mM EDTA, protease and phosphatase inhibitors) and sonicated for 10 s. Nuclear extracts were then clarified by centrifugation at 12 000 rpm at 4°C for 15 min. Total cellular extracts were obtained by sonication in sodium dodecyl sulphate (SDS)/UREA buffer (50 mM TRIS pH 7.5, 2% SDS, 10% glycerol, 100 mM NaF, 6M UREA, 10 mM EDTA). For immunoprecipitation experiments, nuclear extracts were diluted in dilution buffer (50 mM TRIS pH 7.4, 150 mM NaCl, 5 mM EDTA, 10 mM NaF, 0.5% NP40, protease and phosphatase inhibitors) and pre-cleared by incubation with protein A/G conjugated to agarose beads (Thermo Fisher Scientific) for 1 h at 4°C on a rotating wheel. Pre-cleared nuclear extracts were collected by centrifugation and incubated overnight at 4°C on a rotating wheel, with the indicated antibodies. Protein A/G conjugated to agarose beads was then added to the samples and the incubation was continued for an additional hour. Immuno-complexes were collected by centrifugation, washed five-times with dilution buffer and eluted in lithium dodecyl sulphate (LDS) sample buffer (Thermo Fisher Scientific) for WB analyses.

Western blot

Samples were separated by electrophoresis and transferred onto nitrocellulose membranes. After a blocking step in 5% nonfat-dried milk in 0.1% Tween-PBS, membranes were incubated with primary antibodies overnight at 4°C. After three washes in 0.1% Tween-PBS, membranes were incubated with the appropriate HRP-linked secondary antibodies (Bio-Rad) at room temperature for 45 min, washed with 0.1% Tween-PBS and analysed by chemi-luminescence (GE Healthcare Life Science). Images were acquired and quantified using Alliance Mini HD6 system by UVITEC Ltd, Cambridge, equipped with UVI1D Software (UVITEC, 14–630275). Detailed information for all antibodies is provided in Supplementary Table S2.

Nucleoli purification

Nucleoli from HCT116 cells were purified as described by Andersen *et al*. (32). Cytoplasmic, nuclear and nucleolar fractions from equal amounts of cells were subsequently analysed by WB.

Mass-spectrometry

For mass-spectrometry (MS) analysis, RNA pol I subunit RP4194 was immunoprecipitated from nucleolar extracts of HCT116 cells. Immunoprecipitation with normal IgGs was performed as negative control. Co-immunoprecipitated complexes were eluted by incubation in 5% SDS in PBS at 95°C and stored at −80°C prior LC-MS analysis. For details on MS processing see Supplementary Material and Methods.

Sucrose density gradient analysis

Nuclear extracts (200 μg) from HCT116 cells were diluted 1:8 in dilution buffer (50 mM TRIS, pH 7.5, 100 mM NaCl, 10 mM NaF), layered on a linear 10–30% sucrose gradients (in 50 mM TRIS, pH 7.5, 150 mM NaCl, 1.5 mM $MgCl_2$) and subjected to centrifugation for 2 h at 40 000 rpm at 4°C, in a SW60Ti rotor (Beckman Coulter). After centrifugation, fractions of 0.4 ml were collected from top of the gradient, precipitated and resuspended in LDS sample buffer. Equal volumes of each fraction were then analysed by WB.

In vitro pull-down assay

GST fusion proteins were purified from *Escherichia coli* with glutathione-Sepharose beads (GE Healthcare) following standard procedures. For *in vitro* pull-down assay, Che-1 myc expression vector was transcribed and translated *in vitro* using TNT-coupled reticulocyte lysate system (Promega). An equal amount of the translated protein was then incubated with purified GST fusion proteins in interaction buffer (50 mM TRIS pH 7.4, 150 mM NaCl, 0.1 mM EDTA, 0.1% NP40, 100 μg/ml BSA) for 2 h at 4°C on a rotating wheel. At the end of the incubation, the beads were collected by centrifugation and washed five-times with interaction buffer. Bound proteins were eluted in LDS sample buffer, separated on NuPAGE 4–12% precast gels and analysed by WB or visualized by Comassie Blue (Bio-Rad) staining. RPA194-GST-expressing vector was kindly donated by Prof. M.D. Hebert.

Reporter luciferase assay

For luciferase reporter assays, cells were transfected with human rDNA promoter (pHrD-IRES-luc) and siRNA oligonucleotides targeting Che-1 or a control sequence or pHrD-IRES-luc and Che-1-expressing or control vectors. Thirty-six hours after transfection, cells were harvested and lysed in Reporter Lysis Buffer (Promega). Luciferase activity was measured using Luciferase Assay System (Promega) following the manufacturer's protocol and normalized on total protein concentration. pHrD-IRES-luc plasmid was a kind gift from Dr Samson Jacob. Data are presented as mean ± standard deviation (SD) of three independent experiments, performed in triplicate.

RNA isolation and quantitative real-time PCR

Total RNA was isolated from cells using EuroGOLD Tri-Fast reagent (Euroclone) according to the manufacturer's instructions. cDNA was synthesized from equal amount of RNA by reverse transcription using M-MLV reverse transcriptase (Thermo Fisher Scientific) and a mixture of random primers (Thermo Fisher Scientific). This single-stranded cDNA was then used to perform quantitative real-time PCR (qRT-PCR) with specific primers using a SYBR Green 2× qPCR Master Mix (Primerdesign) on a 7500 Fast Real-Time PCR System (Applied Biosystems), following the manufactures' instructions. A melting curve analysis was performed to confirm that single products were amplified and data were processed using the 7500 software v2.0.6 (Applied Biosystems). Relative fold changes were determined by the comparative threshold (ΔΔCT) method (33) using β-actin as endogenous normalization control. Data are presented as mean ± SD of three independent experiments, performed in duplicate. Specific primers employed in qRT-PCR amplifications are listed in Supplementary Table S3.

Chromatin immunoprecipitation assay

Chromatin immunoprecipitation (ChIP) experiments were performed as previously described by Bruno *et al*. (29) using the following antibodies: anti-AATF/Che-1 (Bethyl), anti-UBF (H-300; Santa Cruz Biotechnology), anti-RPA194 (H-300; Santa Cruz Biotechnology), anti-HDAC1 (Sigma-Aldrich), anti-H3K9me3 (Abcam), anti-H3K27Ac (Millipore) and anti-H4Ac (Millipore). For sequential ChIP experiments (Re-ChIP), immunoprecipitated complexes were eluted in 25 μl 10 mM DTT for 30 min at 37°C. After centrifugation, the supernatant was diluted 10 times in Re-ChIP buffer (1% Triton X-100, 2 mM EDTA, 150 mM NaCl, 20 mM TRIS pH 8.0) and subjected again to ChIP procedures. Immunoprecipitations with no specific immunoglobulins (Santa Cruz Biotechnology) were performed as negative controls. For quantitative ChIP analysis (ChIP-qRT), 1 μl of purified DNA was used for amplification on a 7500 Fast Real-Time PCR System (Applied Biosystems) using a SYBR Green 2× qPCR Master Mix (Primerdesign). Information on primers used in these experiments is provided in Supplementary Table S3.

Protein synthesis assay

Global protein synthesis was assessed by puromycin incorporation as described in Schmidt *et al*. (34). Briefly, cells depleted or not for Che-1 expression were pulsed for 10 min with 10 μg/ml puromycin and chased for 30 min at 37°C in a humidified atmosphere with 5% CO_2. Total cellular extracts were then analysed by WB using an anti-puromycin antibody.

Statistical analysis

Data are presented as mean of three independent experiments ± SD. Statistical analyses were performed using R software. Two-tailed Student's *t*-tests with Benjamini–Hochberg correction were performed to compare one parameter between two groups. For multiple group comparison, one-way ANOVA with Tukey HSD test was used. $P < 0.05$ was considered significant. Statistical significance is indicated by asterisks as follows: $*P < 0.05$, $**P < 0.01$, $***P < 0.005$, $****P < 0.001$, n.s. = not significant.

MS data analysis

All mass spectrometric raw data were processed with Maxquant (version 1.5.3.8) using default parameters (35). Briefly, MS2 spectra were searched against the Uniprot HUMAN.fasta (downloaded 16.6.2017) database, including a list of common contaminants. False discovery rates on protein and PSM level were estimated by the target-decoy approach to 1% (Protein FDR) and 1% (PSM FDR) respectively. The minimal peptide length was set to seven amino acids and carbamidomethylation at cysteine residues was considered as a fixed modification. Oxidation (M) and Acetyl (Protein N-term) were included as variable modifications. The match-between runs option was enabled. LFQ quantification was enabled using default settings. Maxquant output files were further processed using Perseus (version 1.6.10.0). Obtained protein iBAQs intensities were $\log_2$ transformed. Proteins flagged as 'only identified by site', 'reverse' and 'potential contaminant' were removed from the data set. In total, four biological replicates were analysed (no technical replicates). The proteins list was filtered for a minimum of three measured values in at least one group (control, or IP), and then the missing values were imputed from a normal distribution. Statistical significance of putative IP RNA pol I interactors was assessed using a two-sided *t*-test (fudge factor S0 = 1) (36), followed by the permutation–based method to determine q-values (FDR < 0.05).

RESULTS

Che-1 interacts with RNA pol I transcription machinery and binds to rDNA

Che-1 is a nucleolar protein involved in ribosomal RNA maturation and proposed as a structural component of the small subunit (SSU) processome, the ribonucleoprotein complex required for the early steps of pre-rRNA processing (27). The SSU processome assembles co-transcriptionally on pre-rRNA, and several factors of this complex are also required for optimal rDNA transcription (37). This evidence, along with the ability of Che-1 to regulate RNA pol II-dependent transcription, prompted us to investigate the potential role of this protein in the transcription of ribosomal RNA genes. Our first step was to verify whether Che-1 could be a component of the RNA pol I machinery. To this aim, we performed co-immunoprecipitation experiments coupled to mass spectrometry analysis in order to characterize the protein interactome of the largest subunit (RPA194) of this enzyme. This analysis allowed us to identify 180 proteins significantly enriched in RPA194 precipitates (Supplementary Table S1). As expected, RPA194 interactome contains many subunits of RNA pol I holoenzyme, proteins involved in pre-rRNA processing and many known regulators of ribosomal gene transcription, such as nucleolar factor UBF

(Figure 1A). Notably, we were also able to identify Che-1 as a novel RNA pol I-interacting factor. To validate these results, we performed co-immunoprecipitation experiments with nuclear extracts of HCT116 cells. As shown in Figure 1B, Che-1 was detected in both RNA pol I and UBF precipitates, thus indicating an interaction between these proteins. Furthermore, these interactions were also confirmed in reciprocal co-immunoprecipitation experiments (Supplementary Figure S1A) and by PLA, in which protein–protein interactions are visualized as discrete spots by fluorescence microscopy (Figure 1C). Consistent with their presence in the same complex, Che-1, RNA pol I (RPA194 subunit) and UBF, showed similar sedimentation behaviour in a sucrose gradient analysis (Figure 1D), and immunofluorescence analysis showed that Che-1 largely co-localizes with both proteins within the nucleolus of HCT116 cells (Supplementary Figure S1B). Since Che-1 has been recently identified as a pre-rRNA binding protein (38,39), we performed co-immunoprecipitation experiments using nuclear extracts of HCT116 cells treated or not with RNAse A, to rule out the possibility that pre-rRNA could mediate Che-1 association with the transcription machinery. These experiments revealed that RNA removal does not abrogate the binding of Che-1 to RNA pol I and UBF, demonstrating the specificity of these interactions (Figure 1E). In addition, pull-down experiments with recombinant glutathione S-transferase RPA194 (RPA194-GST) and *in vitro* translated Che-1 myc revealed a direct interaction between these two proteins (Supplementary Figure S1C). Next, to assess whether Che-1 was also able to associate with ribosomal RNA genes (rDNA), we carried out ChIP assays with an antibody against Che-1. Real-time analysis of the immunoprecipitated DNA using primer pair sets spanning the entire human rDNA repeat, enabled us to generate a profile of Che-1 binding throughout this locus. In this way, we found that Che-1 is associated with rDNA across the entire length of the repeat, but it is particularly enriched at the promoter region (H42.9) (Figure 1F). Importantly, control ChIP with a non-specific antibody did not show any significant enrichment. Finally, sequential ChIP (Re-ChIP) performed with antibodies against RNA pol I or UBF (first round) followed by immunoprecipitation with anti-Che-1 antibody (second round), showed that Che-1 is enriched at both RNA pol I and UBF-occupied rDNA promoter (Figure 1G), indicating that these proteins bind simultaneously to rDNA as parts of the same complex. Overall, the ability of Che-1 to interact with RNA pol I and UBF, along with its binding to rDNA strongly indicate a functional role for this protein in rDNA transcription.

Che-1 promotes rDNA transcription

As already mentioned, ribosomal genes are transcribed as a single polycistronic 47S pre-rRNA, which is rapidly processed to generate mature 18S, 28S and 5.8S rRNAs. Therefore, to investigate the role of Che-1 in rDNA transcription, we analysed the amount of this short-lived precursor in different cell lines depleted or not for Che-1 expression using quantitative Real Time PCR (qRT-PCR). For these experiments, we used a specific pair set of primers inside the 5′ portion of the 5′ externally transcribed spacer region (5′-ETS), known as leader sequence (Figure 2A), whose cleavage and degradation represent the first steps in pre-rRNA processing (40). As shown in Figure 2B, downregulation of Che-1 by transfection with specific siRNA oligonucleotides (Supplementary Figure S2A) induced a reduction of 47S pre-rRNA levels to about 40–60% compared with the control. Similar results were obtained in cells transfected with a second specific siRNA targeting Che-1 and in engineered HCT116 (shChe-1 HCT116) cells in which Che-1 depletion can be induced by doxycycline (Dox) administration, confirming, in such way, the specificity of this effect (Supplementary Figure S2B and C). However, even though quantification of 47S pre-rRNA levels is considered a sensitive indicator of RNA pol I activity (41), the amount of pre-rRNA inside the cell could also be affected by its stability. For this reason, to confirm that Che-1 effect was indeed exerted at transcriptional level, we directly monitored RNA pol I activity by luciferase assays using the human rDNA promoter (pHrD-IRES-luc) as a reporter (42). These experiments showed that silencing of Che-1 in different cell lines induces a strong inhibition of rDNA promoter activity (Figure 2C and Supplementary Figure S2D and E), thus indicating a direct effect of this protein on RNA pol I machinery. This finding was further confirmed by *in vivo* pulse labelling with the nucleoside analogue 5-FUrd and the analysis of its incorporation into nascent RNA through immunostaining. Indeed, as shown in Figure 2D and Supplementary Figure S2F, cells depleted for Che-1 expression exhibited a reduction of 5-FUrd signal compared with control cells, confirming an inhibition of RNA pol I activity. Conversely, ectopic overexpression of Che-1 induced an increase of both 47S pre-rRNA levels and rDNA promoter activity (Figure 2E and F; Supplementary Figure S2G and H). To characterize the region of Che-1 required for regulating RNA pol I activity, we analysed rDNA promoter activity in cells transfected with Che-1 full length or its partial deletions. These experiments revealed that the Che-1 region spanning amino acids 164–370 is required to promote rDNA transcription, since a mutant lacking this region failed to induce rDNA promoter activity (Supplementary Figure S2I). Interestingly, this region contains the leucine zipper domain that has already been found involved in binding to RNA pol II. Finally, we demonstrated that Che-1, although to a lesser extent, was also able to modulate RNA pol I activity in normal human fibroblasts (Figure 2G and Supplementary Figure S2J and K), suggesting that this protein plays a key role in the maintenance of cellular homeostasis. Altogether, these results indicate that Che-1 modulation affects rRNA synthesis at transcriptional level.

Che-1 affects rDNA epigenetic state and modulates UBF and RNA pol I binding to the rDNA promoter

Next, we attempted to get some mechanistic insights on the role of Che-1 in rDNA transcription. Previous studies have demonstrated this protein's ability to promote RNA pol II-dependent transcription by displacing histone deacetylase (HDAC) HDAC1, from specific transcription factors, thus inducing local histone hyper-acetylation at sites where it is recruited (13,30,43). Since HDAC1 has been described as a repressor of rDNA transcription (11,44), we verified

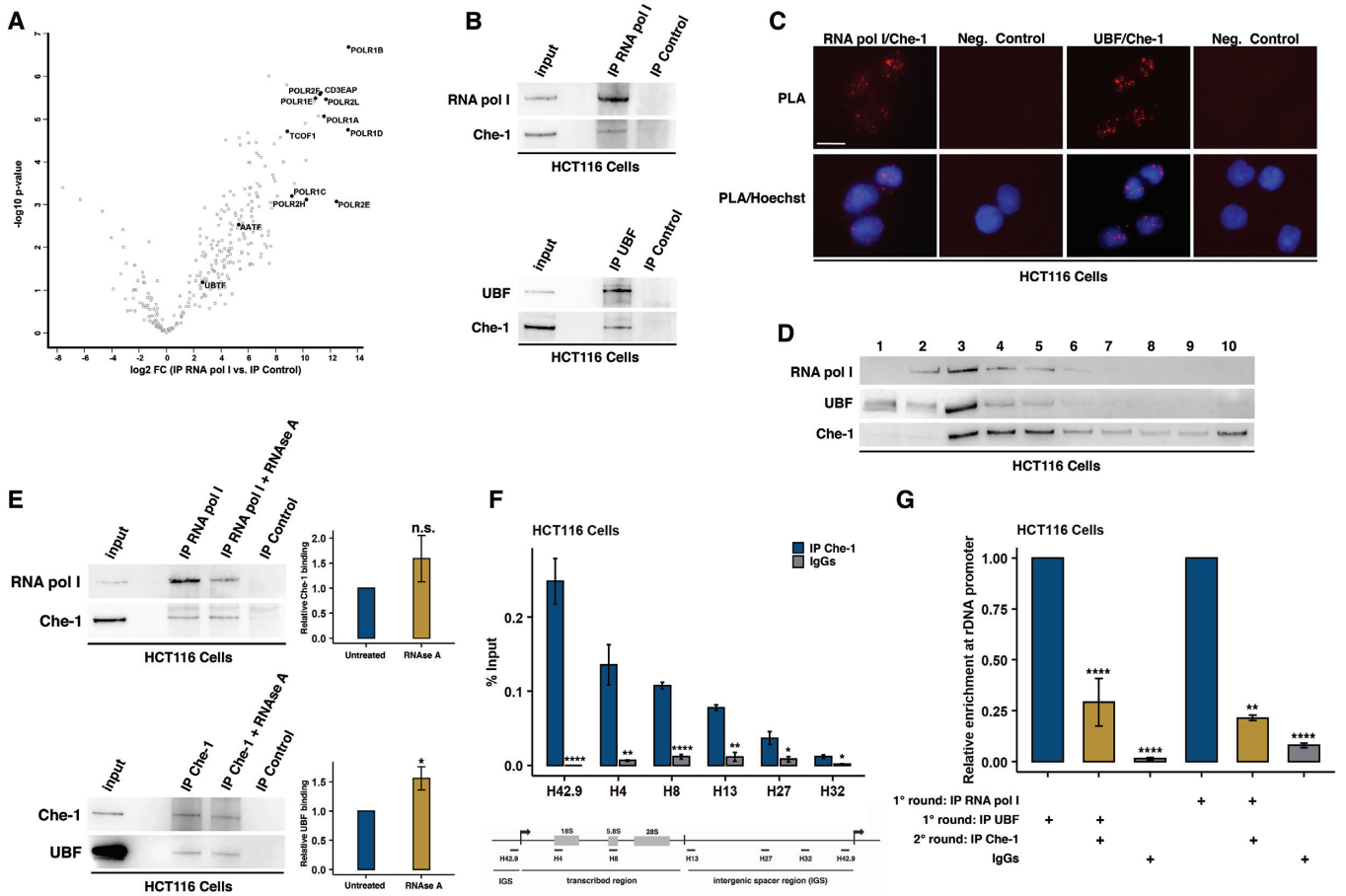

Figure 1. Che-1 interacts with RNA pol I transcription machinery and binds to rDNA. (**A**) Scatter plot of putative RNA pol I interacting proteins. The results of the *t*-test comparison of protein intensities measured via MS are depicted. On the *x*-axis is the mean $\log_2$ difference in intensities of proteins measured in IP RNA pol I (subunit RPA194) versus IP control; on the *y*-axis are the corresponding $-\log_{10}$ *P*-values. In black are indicated the known components of the RNA pol I complex identified in the experiment and the protein Che-1 (AATF). For a complete list of all significant interactors, please refer to Supplementary Table S1. (**B**) Nuclear extracts from HCT116 cells were subjected to immunoprecipitation with either RNA pol I (RPA194 subunit; top) or UBF (bottom) antibodies. Immuno-precipitated complexes were then analysed by WB with the indicated antibodies. Input corresponds to 5% of the nuclear extract used for immunoprecipitation. (**C**) Representative images showing the interaction between either RNA pol I and Che-1 or UBF and Che-1 revealed by PLA. Negative controls were performed by omitting Che-1 primary antibody, whilst nuclei were stained with Hoechst dye. Scale bar, 10 μM. (**D**) Nuclear extracts from HCT116 cells were centrifuged on a linear 10–30% sucrose gradient. Equal volumes of the collected fractions were analysed by WB with the indicated antibodies. (**E**) Left: HCT116 nuclear extracts were immunoprecipitated with either RNA pol I (RPA194 subunit; top) or Che-1 (bottom) antibodies in the presence or absence of RNAse A 20 μg/ml. Immuno-precipitated complexes were then analysed by WB with the indicated antibodies. Input corresponds to 5% of the nuclear extract used for immunoprecipitation. Right: Relative Che-1 binding (top) and UBF binding (bottom) were calculated from three different experiments by densitometry. Che-1 and UBF intensities were normalized to the ones of RNA pol I and Che-1, respectively. (**F**) Top: Che-1 occupancy at rDNA locus was evaluated by ChIP assays with a specific Che-1 antibody in HCT116 cells. The percentage of precipitated DNA was evaluated by real-time PCR with the indicated primer sets and calculated based on the ChIP input. Bottom: Schematic representation of an individual rDNA repeat. (**G**) Re-ChIP experiments were performed in HCT116 cells with the indicated antibodies. The percentage of precipitated DNA was evaluated by real-time PCR with a specific primer set for the H42.9 region and calculated based on the ChIP input. Data are presented as percentage of first round of ChIP. Statistical significance is indicated by asterisks as follows: $*P < 0.05$, $**P < 0.01$, $***P < 0{,}005$, $****P < 0{,}001$, n.s. = not significant. Please also see Supplementary Figure S1.

whether Che-1 could regulate RNA pol I driven transcription by acting as an HDAC1 endogenous inhibitor also at ribosomal gene level. Indeed, luciferase assays performed in 293T cells transfected with rDNA promoter and either HDAC1 or HDAC1 and Che-1 expressing vectors, showed that Che-1 overexpression is able to rescue the inhibition of rDNA promoter activity induced by HDAC1 (Figure 3A). Furthermore, ChIP experiments with an anti-HDAC1 antibody in HCT116 cells depleted or not for Che-1 expression or in shChe-1 HCT116 cells treated with Dox, revealed that the absence of Che-1 leads to accumulation of this histone deacetylase on the rDNA promoter (Figure 3B and C; Supplementary Figure S3A and B). In agreement with these results, analysis of the acetylation state of rDNA by ChIP assays upon Che-1 depletion showed a decrease in the acetylation levels of H3K27 and H4, two modifications associated with transcriptionally active repeats (Figure 3D and Supplementary Figure S3B) (3,45). Notably, silencing of Che-1 was also associated with an increase in the repressing marker H3K9me3 (3), indicating this protein's role in the regulation of the epigenetic state of rRNA genes (Figure 3D and Supplementary Figure S3B). In addition, since

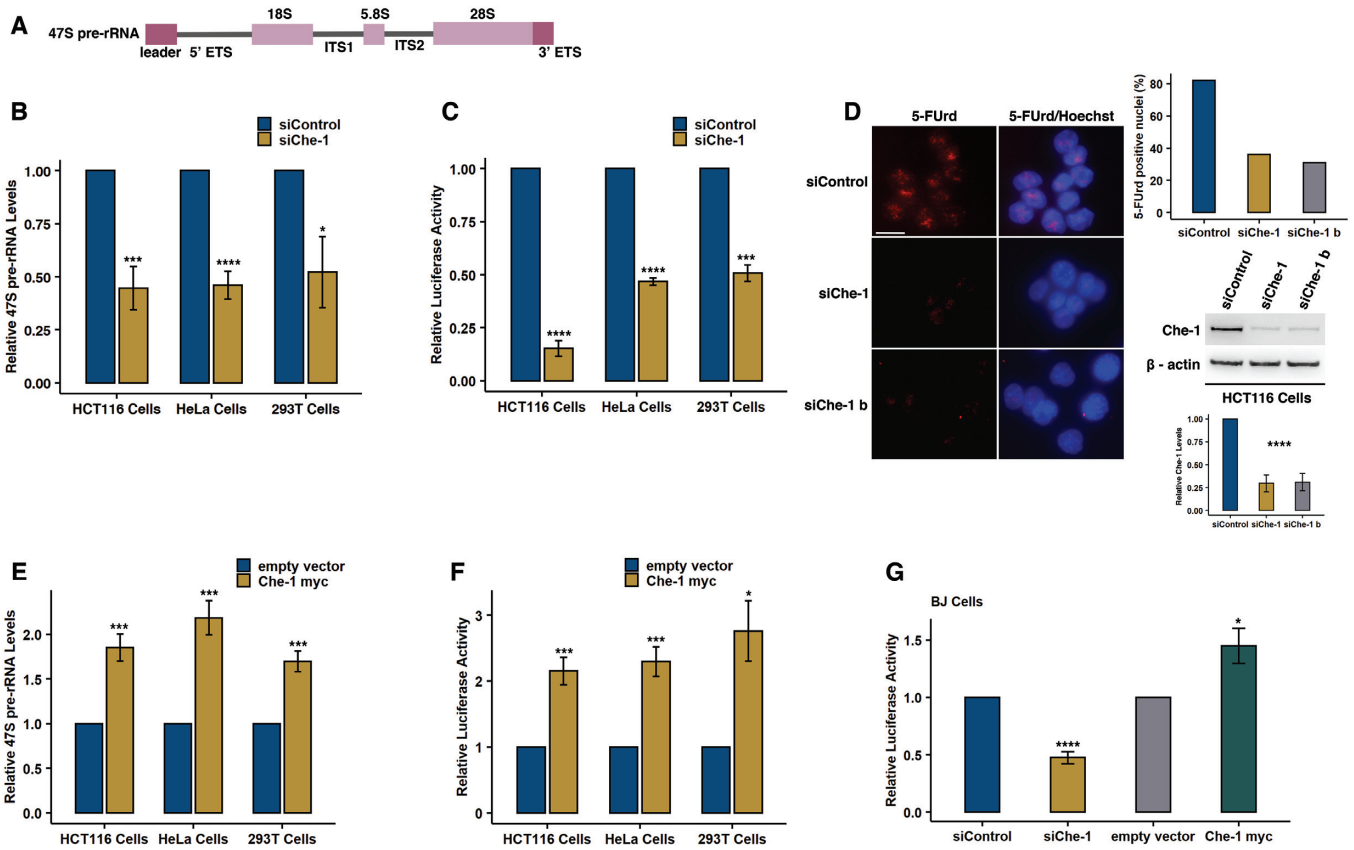

Figure 2. Che-1 promotes rDNA transcription. (**A**) Schematic representation of human 47S pre-rRNA. 5' ETS, 5' external transcribed region; ITS1, internal transcribed region 1; ITS2, internal transcribed region 2; 3' ETS, 3' external transcribed region. (**B**) Real-time PCR (qRT-PCR) analysis of 47S pre-rRNA levels in the indicated cell lines transfected with siRNA oligonucleotides targeting Che-1 (siChe-1) or a control sequence (siControl). Relative fold changes were determined by the comparative threshold (ΔΔCT) method using β-actin as endogenous normalization control. (**C**) Luciferase activity of human rDNA promoter (pHrD-IRES-luc) was measured in the indicated cell lines transfected with pHrD-IRES-luc and siChe-1 or siControl oligonucleotides. (**D**) Left: 5-FUrd labelled RNA was evaluated by immunostaining with anti-BrdU antibody in HCT116 cells transfected with two different siRNA oligonucleotides targeting Che-1 (siChe-1 and siChe-1 b) or a control sequence (siControl). Nuclei were stained with Hoechst dye. Scale bar, 10 μM. Right: bar plot showing the percentage of 5-FUrd positive nuclei (top). Percentage was calculated from 100 randomly selected cells for each group. Representative WB showing the transfection efficiency of the 5-FUrd incorporation assay described above (bottom). The bar plot under the WB shows the average downregulation of Che-1 observed in these experiments ($n = 3$). (**E**) qRT-PCR analysis of 47S pre-rRNA levels in the indicated cell lines transfected with either empty vector or Che-1 expressing vector (Che-1 myc). Relative fold changes were determined by the comparative threshold (ΔΔCT) method using β-actin as endogenous normalization control. (**F**) Luciferase activity of human rDNA promoter was measured in the indicated cell lines transfected with pHrD-IRES-luc along with empty vector or Che-1 expressing vector (Che-1 myc). (**G**) Luciferase activity of human rDNA promoter was measured in BJ human fibroblasts transfected with siChe-1 or siControl oligonucleotides or with empty vector or Che-1 expressing vector (Che-1 myc). All data are expressed as a percentage of control value (siControl/empty vector) and presented as mean ± SD of three independent experiments. Statistical significance is indicated by asterisks as follows: $*P < 0.05$, $**P < 0.01$, $***P < 0.005$, $****P < 0.001$, n.s. = not significant. Please also see Supplementary Figure S2.

Che-1 is an RNA pol I machinery interactor (Figure 1), we evaluated whether it could affect the occupancy of RNA pol I and UBF on rDNA repeats. Thus, we performed ChIP assays using antibodies against RNA pol I and UBF to monitor the enrichment of these proteins on rDNA in HCT116 cells depleted or not for Che-1 expression. As shown in Figure 3E and F and Supplementary Figure S3C and D, Che-1 silencing has opposite effects on RNA pol I and UBF binding to rDNA promoter, inducing an increase of RNA pol I and a concomitant decrease of UBF. This particular pattern of enrichment is similar to the one observed after the depletion of nucleolin, a nucleolar phosphoprotein involved in rDNA transcription elongation (46) and suggests that Che-1 could be also required for this step of the transcriptional process. Overall, these findings indicate that Che-1 regulates rDNA transcription by modulating the epigenetic state of the rRNA gene promoter and by affecting the recruitment of RNA pol I machinery.

Che-1 nucleolar retention is coupled with ongoing rDNA transcription

Residency of nucleolar proteins is very dynamic and subject to constant change in response to different clues (32). Indeed, inhibition of rRNA synthesis has been shown to induce re-localization of many of these proteins to the nucleolar periphery, forming nucleolar caps, or to translocate to the nucleoplasm (47,48). To verify whether nucleolar retention of Che-1 was linked to ongoing rDNA transcription, we monitored its localization following inhibition of rRNA synthesis. To this aim, we performed immunofluorescence analysis on different cell lines treated with actinomycin D

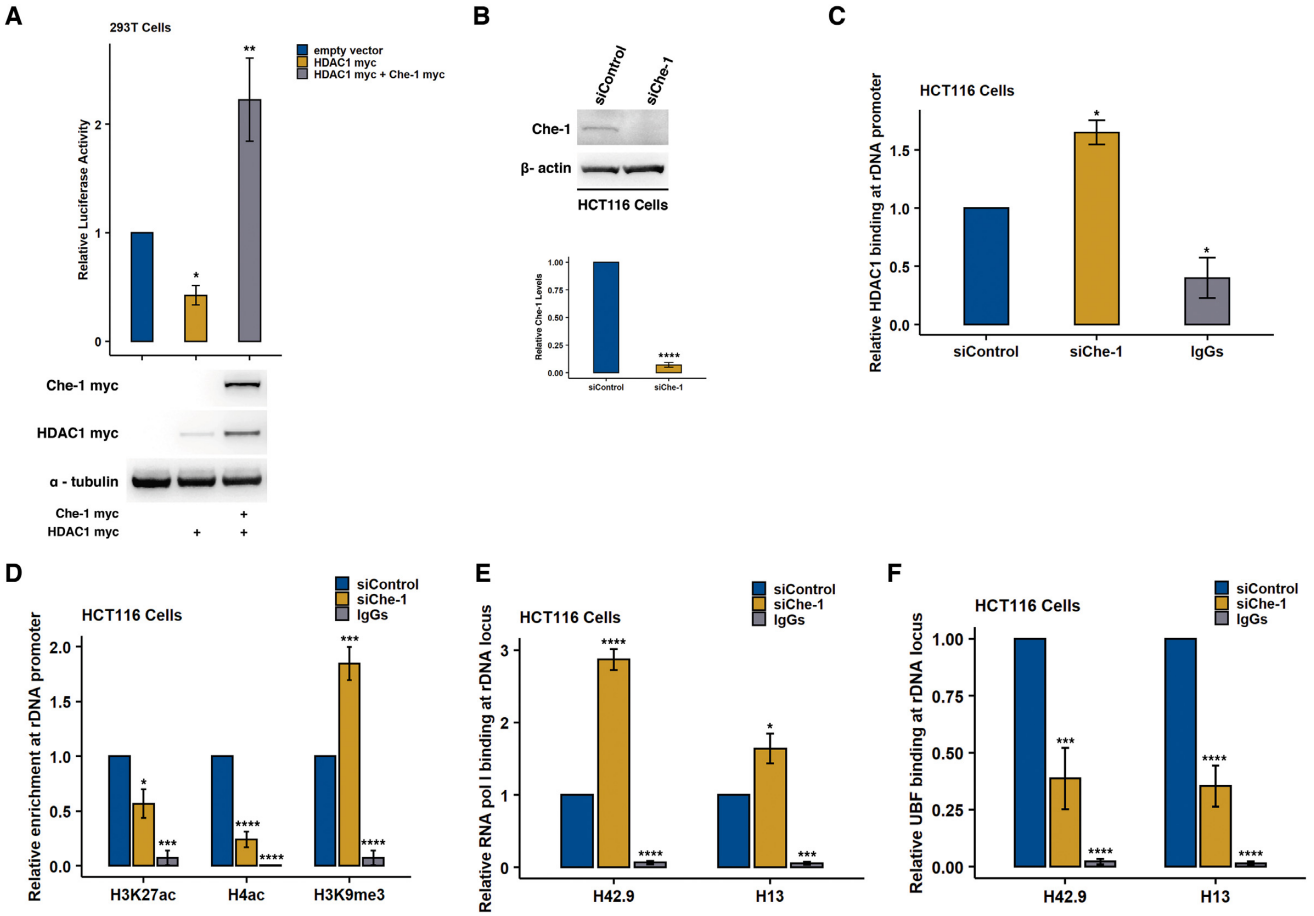

Figure 3. Che-1 affects rDNA epigenetic state and modulates UBF and RNA pol I binding to the rDNA promoter. (**A**) Luciferase activity of human rDNA promoter was measured in 293T cells transfected with pHrD-IRES-luc and either empty vector or HDAC1 expressing vector (HDAC1 myc) alone or in combination with Che-1 expressing vector (Che-1 myc). Data are expressed as a percentage of the control value (empty vector) and presented as mean ± SD of three independent experiments, performed in triplicate (top). WB analysis with the indicated antibodies of representative samples used in the luciferase assay showed above (bottom). (**B**) Representative WB with the indicated antibodies of total cellular extracts from HCT116 cells transfected with siChe-1 or siControl oligonucleotides and simultaneously subjected to the ChIP analyses described below. The bar plot under the WB shows the average downregulation of Che-1 observed in these experiments ($n = 3$). (**C**) HDAC1 occupancy at rDNA promoter was evaluated by ChIP assay with a specific HDAC1 antibody in HCT116 cells depleted or not for Che-1 expression. The amount of precipitated DNA was evaluated by real-time PCR with a specific primer set for the H42.9 region. (**D**) Epigenetic state of rDNA promoter was evaluated by ChIP assays with the indicated antibodies in HCT116 cells depleted or not for Che-1 expression. The amount of precipitated DNA was evaluated by real-time PCR with a specific primer set for the H42.9 region. RNA pol I (**E**) and UBF (**F**) occupancy at rDNA locus was evaluated by ChIP assays with specific RNA pol I or UBF antibodies in Che-1-depleted HCT116 cells. The amount of precipitated DNA was evaluated by real-time PCR with the indicated primer sets and calculated based on the ChIP input. ChIP assays with non-specific IgG were used as negative control in all experiments. All data are expressed as a percentage of control value (siControl) and presented as mean ± SD of three independent experiments. Statistical significance is indicated by asterisks as follows: $*P < 0.05$, $**P < 0.01$, $***P < 0.005$, $****P < 0.001$, n.s. = not significant. Please also see Supplementary Figure S3.

(Act. D), an intercalating agent that at low concentration (100 ng/ml) specifically inhibits RNA pol I elongation activity (49), and CX-5461, a small molecule that selectively inhibits RNA pol I recruitment on rDNA promoter (50). These experiments showed that upon inhibition of rDNA transcription Che-1 loses its peculiar nucleolar staining displaying a more diffuse nuclear localization, especially evident in Act. D-treated cells (Figure 4A and Supplementary Figure S4A). Similar results were obtained in response to treatment with other compounds known for their ability to affect rRNA synthesis (Supplementary Figure S4B) (51–53). As expected, these treatments also induced RNA pol I redistribution, thus impairing co-localization and association of the two proteins (Figure 4A and B; Supplementary Figure S4A and C). Not surprisingly, interaction between Che-1 and transcription factor UBF was also affected by inhibition of rDNA transcription (Figure 4B). In agreement with these results, ChIP experiments showed that inhibition of RNA pol I activity, confirmed by qRT-PCR quantification of 47S pre-rRNA levels (Figure 4C and Supplementary Figure S4D), strongly affected Che-1 recruitment onto the rDNA promoter (Figure 4D and Supplementary Figure S4E). Importantly, loss of Che-1 binding was associated with a concomitant increase of HDAC1 recruitment and a reduction of histone acetylation at rDNA promoter (Figure 4D). In addition, since nucleolar factors can be tethered in the nucleolus by interactions with nucleolar RNA (54), we examined whether Che-1 localization was dependent on its

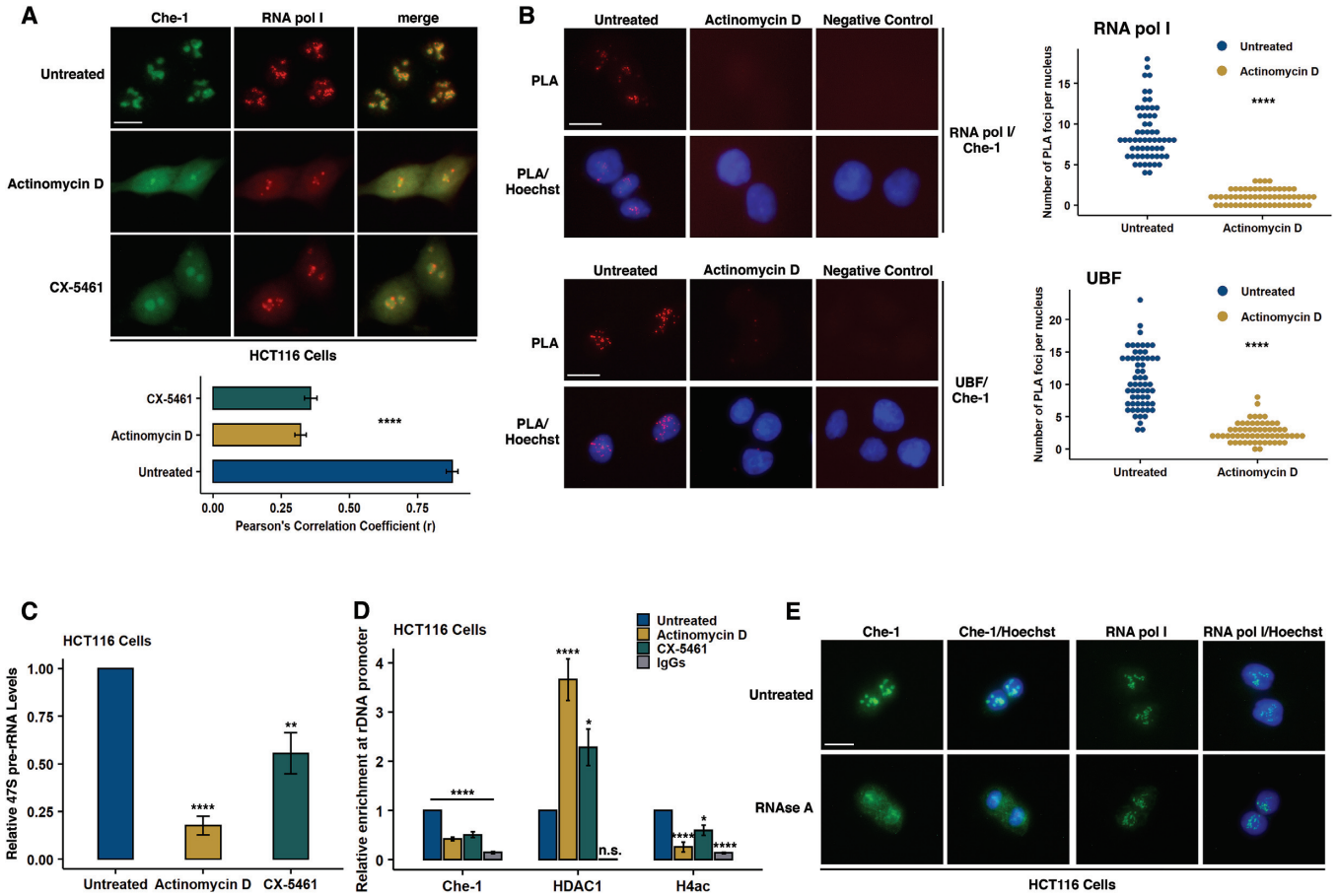

Figure 4. Che-1 nucleolar retention is coupled with ongoing rDNA transcription. (**A**) Representative immunofluorescence images of HCT116 cells treated or not with RNA pol I transcription inhibitors Actinomycin D (100 ng/ml for 6 h) or CX-5461 (1 μM for 16 h) and co-immunostained with Che-1 and RNA pol I (RPA194 subunit) antibodies. Scale bar, 10 μM (top). Co-localization between Che-1 and RNA pol I was quantified by calculating the Pearson's correlation coefficient (r) from 10 randomly selected cells for each group (bottom). (**B**) Left: Representative images of PLA, showing the interaction between RNA pol I and Che-1 (top) or UBF and Che-1 (bottom) upon Actinomycin D treatment. Negative controls were performed by omitting Che-1 primary antibody whilst nuclei were stained with Hoechst dye. Scale bar, 10 μM. Right: box plots showing the number of PLA foci per nucleus ($n = 60$ cells for each group). (**C**) qRT-PCR analysis of 47S pre-rRNA levels in HCT116 cells treated as in A. Relative fold changes were determined by comparative threshold (ΔΔCT) method using β-actin as endogenous normalization control. Data are presented as mean ± SD of three independent experiments. (**D**) Che-1, HDAC1 and H4 acetylated enrichments at rDNA promoter were evaluated by ChIP assays with specific antibodies in HCT116 cells treated as in A. The percentage of precipitated DNA was evaluated by real-time PCR with a specific primer set for the H42.9 region and calculated based on the ChIP input. Data are expressed as a percentage of control value (untreated) and presented as mean ± SD of three independent experiments. (**E**) Representative immunofluorescence images of HCT116 cells immunostained with Che-1 or RNA pol I antibody. Before staining, pre-permeabilized cells were treated, or not, with RNAse A 1 mg/ml for 10 min at room temperature. Nuclei were counterstained with Hoechst dye. Scale bar, 10 μM. Statistical significance is indicated by asterisks as follows: $*P < 0.05$, $**P < 0.01$, $***P < 0.005$, $****P < 0.001$, n.s. = not significant. See also Supplementary Figure S4.

ability to bind RNA. Indeed, we found that treatment of pre-permeabilized cells with RNAse A leads to releasing of Che-1 from nucleoli, thus indicating that RNA is required for nucleolar retention of this protein (Figure 4E). Altogether, these results indicate that active rDNA transcription and binding to ribosomal RNA underlie Che-1 nucleolar localization.

Che-1 depletion induces aberrant nucleolar morphology

Active rDNA transcription is fundamental for proper nucleoli assembly and integrity (55,56), and the tight relationship between transcription and structure within nucleoli is proven by the observation that depletion of rDNA transcription regulators can be associated with changes in nucleolar number and morphology (57–59). For this reason, we verified whether Che-1, beside its role in rDNA transcription, could also be involved in the regulation of the nucleolar structure. To do this, nucleolar morphology was analysed by immunostaining for fibrillarin, a widely used nucleolar marker, on cells depleted or not for Che-1 expression by transfection with siRNA oligonucleotides. Immunostaining for Che-1 or WB analyses were used to verify the efficiency of this downregulation. These experiments revealed that whilst control cells contain two to three nucleoli, Che-1-depleted cells mainly display only one large rounded nucleolus per cell (Figure 5A and Supplementary Figure S5A and B). This phenotype was also confirmed by detecting nucleoli with a specific dye selective for RNA (Figure 5B and Supplementary Figure S5C). Interestingly, immunoflu-

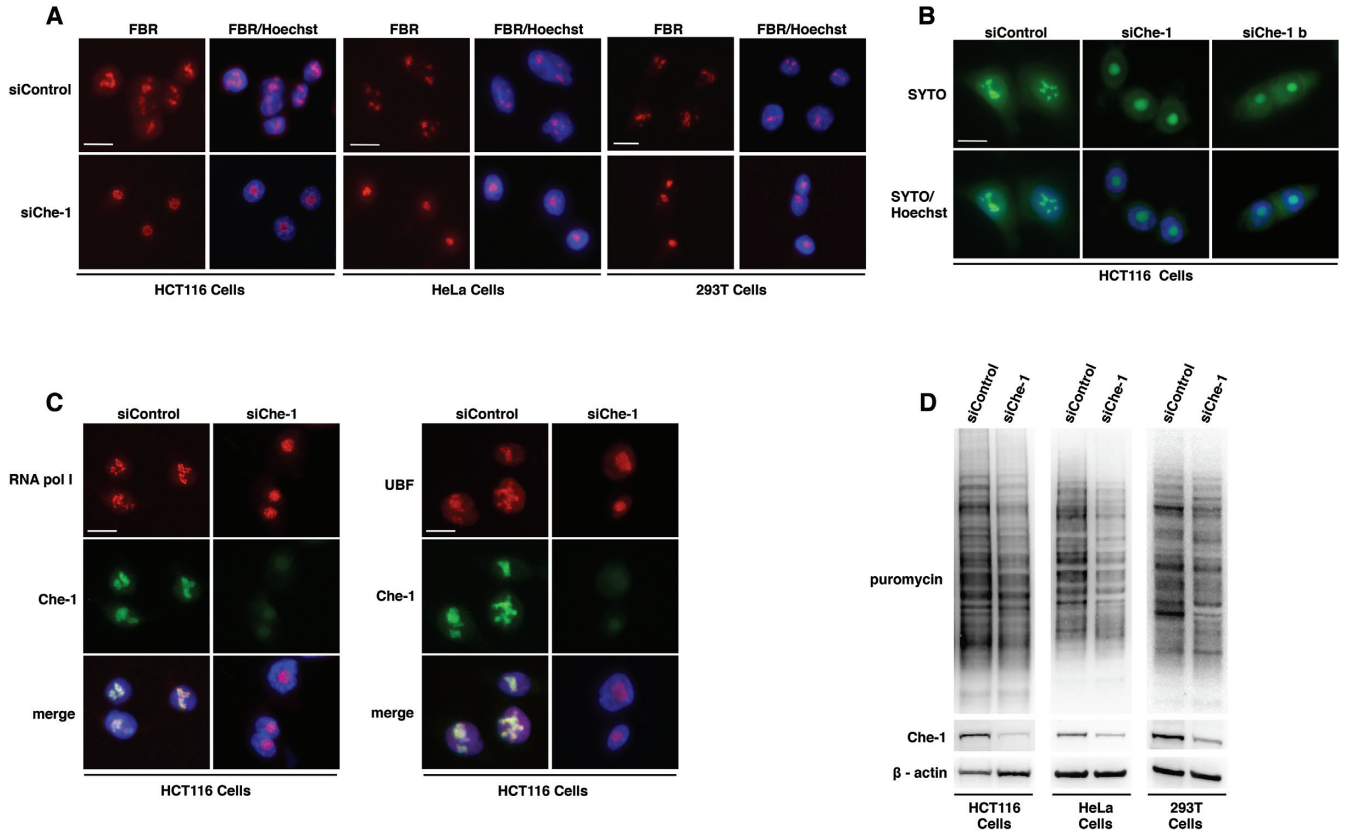

Figure 5. Che-1 depletion induces aberrant nucleolar morphology. (**A**) Representative immunofluorescence images of the indicated cell lines transfected with siChe-1 or siControl oligonucleotides. Cells were stained with anti-fibrillarin antibody (FBR) whilst nuclei were counterstained with Hoechst dye. Scale bar, 10 μM. (**B**) Representative images of HCT116 cells transfected with two different siRNA targeting Che-1 (siChe-1 and siChe-1 b) or a control sequence (siControl) and stained with SYTO RNAselect Green Fluorescent Cell Stain (SYTO), a specific dye for RNA, to detect nucleoli. Nuclei were counterstained with Hoechst dye. Scale bar, 10 μM. (**C**) Representative immunofluorescence images of HCT116 cells transfected as in A. Cells were co-stained with RNA pol I (subunit RPA194) and Che-1 (left) or UBF and Che-1 (right) antibodies whilst nuclei were counterstained with Hoechst dye. Scale bar, 10 μM. (**D**) Representative images of SunSET assays showing global protein synthesis rate upon Che-1 depletion. Total cellular extracts of the indicated cells lines transfected as in A and pulsed with puromycin were analysed by WB with an anti-puromycin antibody to evaluate puromycin-labelled peptides. β-actin was used as loading control. See also Supplementary Figure S5.

orescence analysis performed with antibodies against RNA pol I and UBF showed that Che-1 depletion also leads to a global re-localization of these factors within the nucleolus, thus indicating a role for this protein in the maintenance of nucleolar integrity (Figure 5C and Supplementary Figure S5D). In addition, since rDNA transcription is the rate-limiting step in ribosome biogenesis and hence in the translation capacity of the cells, we tested whether Che-1 depletion could affect global protein synthesis. To do this, we performed SUnSET assays, where the incorporation of puromycin into newly synthesized proteins is used as a read out of global levels of protein synthesis (34). Cells transfected with siChe-1 or siControl oligonucleotides, or shChe-1 HCT116 cells treated with Dox, were pulsed with puromycin and subsequently analysed by WB with an anti-puromycin antibody. As shown in Figure 5D and Supplementary Figure S5E and F, Che-1 depleted cells showed a significant decrease in puromycin incorporation compared to control cells, thus indicating that Che-1 loss is indeed associated with a reduction in protein synthesis in all analysed cell lines.

DNA damage induces a phosphorylation-dependent redistribution of Che-1

It has been demonstrated that many kinds of cellular stress, including DNA damage, block RNA pol I transcription and induce redistribution of nucleolar components (47). To investigate the effects of DNA damage on Che-1 nucleolar localization, we performed an immunofluorescence analysis in HCT116 cells following treatment with the DNA damaging agents Adr or UVB irradiation. These experiments revealed that in contrast to control cells, where Che-1 is mainly localized in the nucleolus along with RNA pol I and UBF, upon DNA damage HCT116 cells exhibit a more diffuse distribution of this protein, associated with the loss of co-localization with both RNA pol I and UBF (Figure 6A and Supplementary Figure S6A). Similar patterns were also observed in 293T and HeLa cells following Adr treatment (Supplementary Figure S6B and C), suggesting a redistribution of Che-1 from nucleolus to nucleoplasm upon DNA damage. Indeed, WB analysis of cytoplasmic, nuclear and nucleolar fractions of HCT116 cells treated or not with Adr, showed a change in the distribution of Che-1 within the

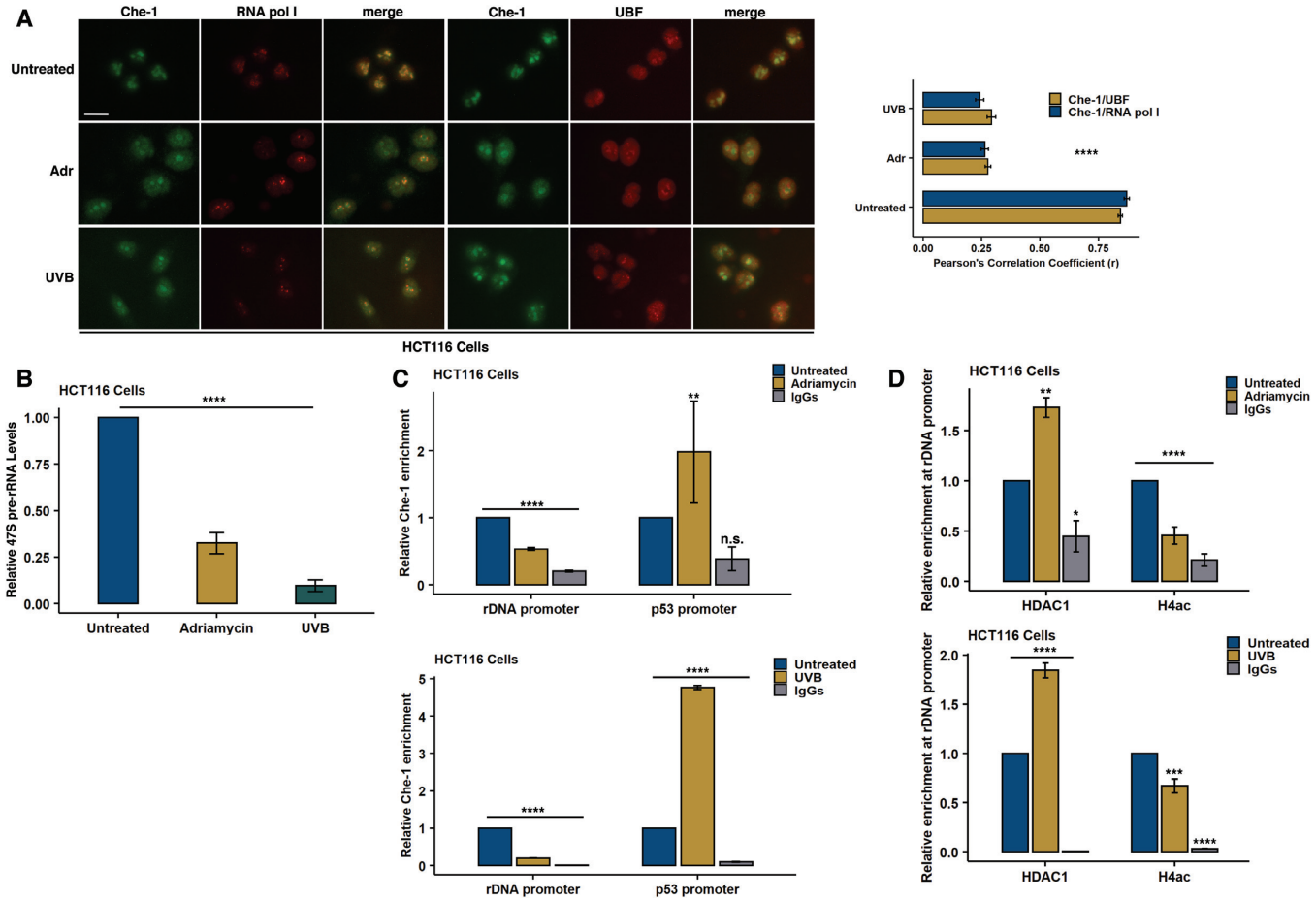

Figure 6. DNA damage induces redistribution of Che-1 from nucleolus to nucleoplasm. (**A**) Representative immunofluorescence images of HCT116 cells treated or not with Adriamycin (1 μM for 4 h) or exposed to UVB irradiation (25 mJ/cm^2). Cells were co-immunostained with Che-1 and RNA pol I (subunit RPA194) or Che-1 and UBF antibodies. Scale bar, 10 μM (left). The co-localization between Che-1 and RNA pol I and between Che-1 and UBF was quantified by calculating the Pearson's correlation coefficient (r) from 10 randomly selected cells for each group (right). (**B**) qRT-PCR analysis of 47S pre-rRNA levels in HCT116 treated as in A. Relative fold changes were determined by the comparative threshold (ΔΔCT) method using β-actin as endogenous normalization control. Data are presented as mean ± SD of three independent experiments. (**C**) Che-1 occupancy at rDNA and *TP53* promoters was evaluated by ChIP assay with a specific Che-1 antibody in HCT116 cells treated as in A. The amount of precipitated DNA was evaluated by real time PCR with a specific primer set for the H42.9 region and calculated relative to the ChIP input. Data are expressed as a percentage of control value (untreated) and presented as mean ± SD of three independent experiments. (**D**) HDAC1 and H4 acetylated (H4ac) enrichments at rDNA promoter were evaluated with specific antibodies in HCT116 cells treated as in A. The amount of precipitated DNA was evaluated by real time PCR with a specific primer set for the H42.9 region and calculated relative to the ChIP input. Data are expressed as a percentage of control value (untreated) and presented as mean ± SD of three independent experiments. Statistical significance is indicated by asterisks as follows: $*P < 0.05$, $**P < 0.01$, $***P < 0.005$, $****P < 0.001$, n.s. = not significant. See also Supplementary Figure S6.

cell, with an increase of this protein in the nuclear fraction and a concomitant decrease in the nucleolar one in treated cells (Supplementary Figure S6D). Of note, these data are in line with already published results showing a redistribution of Che-1 from nucleolus to nucleoplasm upon UV irradiation (24). In agreement with these findings, we showed that DNA damage, in addition to a reduction in 47S pre-rRNA levels (Figure 6B and Supplementary Figure S6E), induces a strong decrease of Che-1 enrichment on the rDNA promoter associated with a concomitant increase of its occupancy on the promoters of genes involved in DNA damage response, such as *TP53*, *p21* and *GADD45* (Figure 6C and Supplementary Figure S6F and G). Interestingly, both Adr treatment and UVB irradiation also induced an accumulation of HDAC1 on rDNA promoter and a decrease of histone acetylation level at this region (Figure 6D). Previous studies have indicated Che-1 as a component of the DNA damage response where phosphorylation by checkpoint kinase ATM plays a pivotal role in the regulation of this protein's activity. Indeed, this modification induces Che-1 re-localization from the promoters of genes involved in cell-cycle progression to the *TP53* promoter, thus inducing *TP53* transcription and cell-cycle arrest (19). Based on this evidence, along with the observation that ATM acts as an inhibitor of rRNA synthesis (60,61), we investigated whether ATM may be involved in regulating Che-1 redistribution and binding to rDNA in response to DNA damage. To this aim, intracellular localization of Che-1 was analysed by immunofluorescence in HCT116 cells exposed to Adr after a pre-treatment with the specific ATM inhibitor caffeine or with the Chk1 inhibitor, LY2603618, as a control. As shown in Figure 7A, caffeine, in contrast to LY2603618,

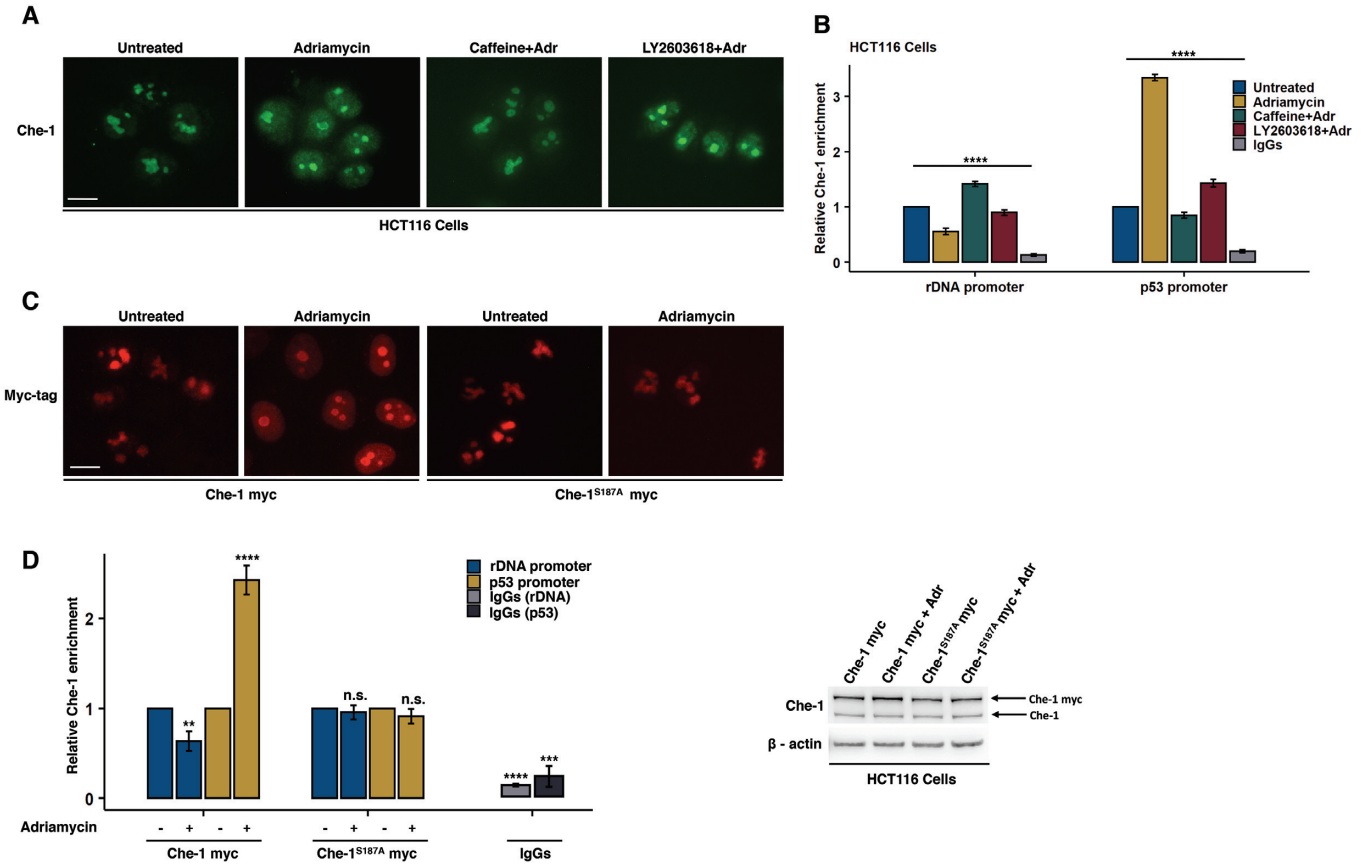

Figure 7. Phosphorylation by ATM regulates Che-1 nucleolar residency. (**A**) Representative immunofluorescence images of HCT116 cells treated or not with Adriamycin (1 μM for 4 h) and immunostained with Che-1 antibody. Where indicated cells were pre-treated with Caffeine (10 mM for 30 min) or with LY2603618 (0.5 μM for 16 h). Scale bar, 10 μM. (**B**) ChIP assays with a specific Che-1 antibody in HCT116 cells treated as in A. The amount of precipitated DNA was evaluated by real-time PCR and calculated relative to the ChIP input. Data are expressed as a percentage of control value (untreated) and presented as mean ± SD of three independent experiments. (**C**) Representative immunofluorescence images of HCT116 cells transfected with the indicated expression vectors and treated with Adriamycin (1 μM for 4 h). Cells were stained with a myc-tag antibody to detect only the exogenous proteins. Scale bar, 10 μM. (**D**) Left: HCT116 cells transfected as in C were subjected to ChIP assays with a myc-tag antibody. The enrichment of the ectopic proteins on rDNA and *TP53* promoters was determined by real-time PCR and calculated based on the ChIP input. Data are expressed as a percentage of control values (Che-1 myc or Che-1^{S187A} myc) and presented as mean ± SD of three independent experiments. Right: WB analysis with the indicated antibodies of representative samples used in the ChIP assay showed on the left. Statistical significance is indicated by asterisks as follows: $*P < 0.05$, $**P < 0.01$, $***P < 0.005$, $****P < 0.001$, n.s. = not significant. Please also see Supplementary Figure S6.

inhibited the redistribution of Che-1 from nucleolus to nucleoplasm induced by Adr treatment, suggesting that phosphorylation by ATM regulates Che-1 nucleolar retention upon DNA damage. In line with these results, ChIP-qRT experiments showed that caffeine was also able to counteract Che-1 re-localization from the rDNA to the *TP53* promoter (Figure 7B and Supplementary Figure S6H). However, in this case, the enrichment of Che-1 on *TP53* promoter induced by DNA damage was partially affected by inhibition of Chk1, suggesting that other phosphorylations may contribute to this particular event. To strengthen these results, we took advantage of a Che-1 mutant (Che-1^{S187A} myc) lacking the ATM phosphorylation site (19). As shown in Figure 7C, in response to Adr treatment, wild-type Che-1 myc displayed a widespread distribution within the nucleus, whilst Che-1^{S187A} myc retained its nucleolar localization. Moreover, in untreated cells, both proteins, Che-1 myc or Che-1^{S187A} myc mutant, were enriched on the rDNA promoter, whilst in response to DNA damage, wild-type Che-1 myc relocated from the rDNA to the *TP53* promoter whereas mutant Che-1^{S187A} myc remained associated with rDNA (Figure 7D). These data collectively support a model in which, upon DNA damage, ATM-dependent redistribution of Che-1 contributes to cell-cycle arrest by reducing rDNA transcription and promoting *TP53* activation.

DISCUSSION

Che-1 is a transcriptional cofactor involved in a wide range of cellular pathways regulating proliferation and survival, in both physiological and pathological conditions. Although its nucleolar localization has been known for many years, only in recent times, its nucleolar functions have started to be investigated. Previous studies have demonstrated an essential role for Che-1 in the early steps of pre-rRNA processing and ribosome maturation, as well as its ability to bind pre-rRNA. Here, we report a novel function of Che-1 in ribosome biogenesis mediated by its ability to regulate

RNA pol I-dependent transcription. We demonstrated that Che-1 interacts with RNA pol I machinery and promotes rRNA synthesis. Notably, Che-1/RNA pol I interaction only occurs during active transcription and is not mediated by pre-rRNA, since treatment with RNAse A did not abrogate this association. Furthermore, we showed that Che-1 binds to rDNA and modifies the epigenetic state of rDNA promoter by modulating the recruitment of HDAC1. Notably, we provided evidence that the decrease in rRNA synthesis induced by Che-1 depletion is associated with aberrant nucleolar morphology and with a reduction in global protein synthesis. Finally, we showed that Che-1 nucleolar retention is linked to active rDNA transcription, and that DNA damage, whilst reducing RNA pol I activity, leads to a redistribution of this protein from nucleolus to nucleoplasm, that is dependent on phosphorylation by checkpoint kinase ATM.

Che-1 was originally identified as an RNA polymerase II binding protein through its interaction with subunit RPB14 (12). Here, we showed that Che-1 is part of the protein interactome of the largest subunit of RNA pol I, RPA194. Interestingly this association is not mediated by subunit AC19, the RNA polymerase I counterpart of RPB14 (62), but relies on a direct association with RPA194 itself.

Consistent with its role in RNA pol I-driven transcription, we found that Che-1 is associated with rDNA. In particular, ChIP analysis revealed a binding of this protein throughout the entire length of the rDNA repeat with a higher enrichment at the promoter, suggesting a possible role for Che-1 in both the initiation and the elongation steps of transcription. To support this hypothesis, we demonstrated that depletion of Che-1 generates an accumulation of RNA pol I at the promoter region, comparable to the one obtained after transcription elongation inhibition (46). Interestingly, Che-1 association to rDNA was also detected in the intergenic spacer region (IGS), now recognized as complex transcriptional units for several IGS non-coding RNA (63), opening the possibility of an involvement of Che-1 also in the regulation of intergenic transcription.

We have previously demonstrated that Che-1 induces histone acetylation and transcription at specific gene promoters by displaying HDAC1 from transcription factors Rb and Sp1 (13). In line with these results, we reported here that Che-1 depletion is associated with an increase of HDAC1 recruitment on rDNA promoter as well as a reduction in histone acetylation and a concomitant increase in H3K9 trimethylation, a known marker of epigenetic silencing, at this region. The precise molecular mechanisms underlying the ability of Che-1 in modifying the epigenetic state of rDNA are not yet clear and need to be elucidated. However, since Che-1 has already been indicated as a component of complexes containing acetyltransferases (64), it is possible that it could modulate histone modifications, not only by acting as an HDAC1 inhibitor, but also by regulating this class of enzymes. Furthermore, given that UBF is a key regulator of rDNA chromatin structure, the involvement of Che-1/UBF interaction in maintaining an active chromatin state could not be excluded.

Pre-rRNA synthesis and processing are two tightly coupled events and many processing factors are indeed required for optimal rDNA transcription (37,65). Since Che-1 has already been indicated as a possible structural component of the SSU processome, acting as a scaffold for proteins and enzymes involved in the processing of pre-rRNA (27), it can be hypothesized that this protein binds to nascent pre-rRNA during transcription and participates in the mechanisms linking rDNA transcription and pre-rRNA processing.

However, regulation of rDNA transcription and processing might not be the only ways in which Che-1 regulates ribosome biogenesis. Indeed, RNA-seq experiments conducted in Che-1-depleted cells revealed the ability of this protein to regulate transcription of many ribosomal proteins (M. Fanciulli, personal communication). Moreover, given its ability to regulate both RNA pol I and pol II activities, it is very likely that Che-1 could also affect the production of 5S rRNA by RNA pol III. If this were the case, Che-1 may contribute to the regulation of ribosome biogenesis also by acting as a central hub for coordinating the activity of all three RNA polymerases.

We provided evidence that phosphorylation of Che-1 by checkpoint kinase ATM regulates its binding to rDNA and its subcellular localization upon DNA damage. However, it is possible that other post-translational modifications may be involved in this phenomenon. For instance, it has been recently demonstrated that in normal growth condition nucleolar acetyltransferase NAT10, whilst promoting rRNA synthesis by acetylating UBF (66), inhibits autophagy induction by interacting with and acetylating Che-1 at lysine 228 (18). More specifically, this modification abolishes the ability of Che-1 to transcriptionally activate mTOR inhibitors Redd1 and Deptor, and it is lost upon energy stress, when NAT10 and Che-1 detach (18). Based on these observations it is reasonable to speculate that acetylation at lysine 228 not only prevents transcriptional activation of Redd1 and Deptor but may also play a role in Che-1 nucleolar localization and in its ability to promote rDNA transcription. A crosstalk between this modification and phosphorylation by ATM, as well as the involvement of others, cannot also be excluded. In this regard, it is worth pointing out that Che-1 has also been indicated as an interacting partner of SIRT7 (67), a nucleolar deacetylase with a positive role in the regulation of rRNA synthesis (68). Further studies on this subject may dissect the specific post-translational modifications regulating Che-1 nucleolar functions.

As mentioned earlier, Che-1 is involved in many cellular pathways, some of which are also implicated in the regulation of rDNA transcription and ribosome biogenesis. For instance, it has been demonstrated that this protein is a direct target of the oncoprotein c-Myc, and together cooperate in regulating the expression of genes involved in cell-cycle progression (15). Since c-Myc is known to be a master regulator of ribosome biogenesis (69,70), it is possible that the two proteins may cooperate also in regulating rDNA transcription.

Previous studies have demonstrated that Che-1 expression is essential for proliferation and survival. In fact, *Traube* (Che-1 mouse orthologue) knockout mice are embryonically lethal and halt the development at the compacted morula stage, showing a reduced number of cells, as well as ribosomes and polysomes. Notably, in preimplantation mouse embryos, protein synthesis is supported by

maternal ribosomes until the morula stage, when nucleolus maturation occurs (71). Based on these observations, it can be hypothesized that the essential role of Che-1 during proliferation and survival may be due to its ability in promoting rRNA synthesis, hence ribosome biogenesis. In agreement with this hypothesis, we demonstrated that induction of rRNA synthesis by Che-1 is not restricted to cancer cells but also occurs in normal fibroblasts. In this context, it is important to keep in mind that Che-1 expression has been found upregulated in both solid and haematological tumours (13) and this upregulation may be linked to the increased ribosome demand of cancer cells necessary to sustain their higher proliferation rates. Therefore, the ability of Che-1 to promote rDNA transcription could not only explain the essential role of this protein during proliferation and development but also contribute to its pathological role in tumourigenesis. Indeed, malignant transformation is tightly linked to dysregulation in RNA pol I activity and ribosome biogenesis and targeting nucleolar functions represents a new track for the design and development of novel anticancer approaches (72–74). In this context, our data support the possibility that inhibition of Che-1 may provide a new strategy for the development of new targeted cancer treatments.

DATA AVAILABILITY

The mass spectrometry data (Raw data and MaxQuant output) have been deposited to the ProteomeXchange Consortium (http://www.ebi.ac.uk/pride) via the PRIDE (75) partner repository with the dataset identifier PXD018143.

SUPPLEMENTARY DATA

Supplementary Data are available at NAR Online.

ACKNOWLEDGEMENTS

We acknowledge Mrs Tania Merlino for the English language revision of the manuscript. Editorial assistance was provided by Aashni Shah (Polistudium SRL, Milan, Italy).

FUNDING

Italian Association for Cancer Research [15255 to M.F.]. Funding for open access charge: Italian Ministery of Health - Ricerca Corrente 2019.
Conflict of interest statement. None declared.

REFERENCES

1. Hannan,K.M., Sanij,E., Rothblum,L.I., Hannan,R.D. and Pearson,R.B. (2013) Dysregulation of RNA polymerase I transcription during disease. *Biochim. Biophys. Acta*, **1829**, 342–360.
2. Stults,D.M., Killen,M.W., Pierce,H.H. and Pierce,A.J. (2008) Genomic architecture and inheritance of human ribosomal RNA gene clusters. *Genome Res.*, **18**, 13–18.
3. Grummt,I. and Langst,G. (2013) Epigenetic control of RNA polymerase I transcription in mammalian cells. *Biochim. Biophys. Acta*, **1829**, 393–404.
4. Goodfellow,S.J. and Zomerdijk,J.C. (2013) Basic mechanisms in RNA polymerase I transcription of the ribosomal RNA genes. *Subcell Biochem.*, **61**, 211–236.
5. Sharifi,S. and Bierhoff,H. (2018) Regulation of RNA Polymerase I transcription in development, disease, and aging. *Annu. Rev. Biochem.*, **87**, 51–73.
6. Panov,K.I., Friedrich,J.K., Russell,J. and Zomerdijk,J.C. (2006) UBF activates RNA polymerase I transcription by stimulating promoter escape. *EMBO J.*, **25**, 3310–3322.
7. Stefanovsky,V., Langlois,F., Gagnon-Kugler,T., Rothblum,L.I. and Moss,T. (2006) Growth factor signaling regulates elongation of RNA polymerase I transcription in mammals via UBF phosphorylation and r-chromatin remodeling. *Mol. Cell*, **21**, 629–639.
8. Sanij,E., Poortinga,G., Sharkey,K., Hung,S., Holloway,T.P., Quin,J., Robb,E., Wong,L.H., Thomas,W.G., Stefanovsky,V. *et al.* (2008) UBF levels determine the number of active ribosomal RNA genes in mammals. *J. Cell Biol.*, **183**, 1259–1274.
9. Voit,R. and Grummt,I. (2001) Phosphorylation of UBF at serine 388 is required for interaction with RNA polymerase I and activation of rDNA transcription. *Proc. Natl. Acad. Sci. U.S.A.*, **98**, 13631–13636.
10. Hannan,K.M., Brandenburger,Y., Jenkins,A., Sharkey,K., Cavanaugh,A., Rothblum,L., Moss,T., Poortinga,G., McArthur,G.A., Pearson,R.B. *et al.* (2003) mTOR-dependent regulation of ribosomal gene transcription requires S6K1 and is mediated by phosphorylation of the carboxy-terminal activation domain of the nucleolar transcription factor UBF. *Mol. Cell. Biol.*, **23**, 8862–8877.
11. Meraner,J., Lechner,M., Loidl,A., Goralik-Schramel,M., Voit,R., Grummt,I. and Loidl,P. (2006) Acetylation of UBF changes during the cell cycle and regulates the interaction of UBF with RNA polymerase I. *Nucleic Acids Res.*, **34**, 1798–1806.
12. Fanciulli,M., Bruno,T., Di Padova,M., De Angelis,R., Iezzi,S., Iacobini,C., Floridi,A. and Passananti,C. (2000) Identification of a novel partner of RNA polymerase II subunit 11, Che-1, which interacts with and affects the growth suppression function of Rb. *FASEB J.*, **14**, 904–912.
13. Iezzi,S. and Fanciulli,M. (2015) Discovering Che-1/AATF: a new attractive target for cancer therapy. *Front. Genet.*, **6**, 141.
14. Welcker,D., Jain,M., Khurshid,S., Jokic,M., Hohne,M., Schmitt,A., Frommolt,P., Niessen,C.M., Spiro,J., Persigehl,T. *et al.* (2018) AATF suppresses apoptosis, promotes proliferation and is critical for Kras-driven lung cancer. *Oncogene*, **37**, 1503–1518.
15. Folgiero,V., Sorino,C., Pallocca,M., De Nicola,F., Goeman,F., Bertaina,V., Strocchio,L., Romania,P., Pitisci,A., Iezzi,S. *et al.* (2018) Che-1 is targeted by c-Myc to sustain proliferation in pre-B-cell acute lymphoblastic leukemia. *EMBO Rep.*, **19**, e44871.
16. Jing,P., Zou,J., Weng,K. and Peng,P. (2018) The PI3K/AKT axis modulates AATF activity in Wilms' tumor cells. *FEBS Open Bio.*, **8**, 1615–1623.
17. Kumar,D.P., Santhekadur,P.K., Seneshaw,M., Mirshahi,F., Uram-Tuculescu,C. and Sanyal,A.J. (2019) A regulatory role of apoptosis antagonizing transcription factor in the pathogenesis of nonalcoholic fatty liver disease and hepatocellular carcinoma. *Hepatology*, **69**, 1520–1534.
18. Liu,X., Cai,S., Zhang,C., Liu,Z., Luo,J., Xing,B. and Du,X. (2018) Deacetylation of NAT10 by Sirt1 promotes the transition from rRNA biogenesis to autophagy upon energy stress. *Nucleic Acids Res.*, **46**, 9601–9616.
19. Bruno,T., De Nicola,F., Iezzi,S., Lecis,D., D'Angelo,C., Di Padova,M., Corbi,N., Dimiziani,L., Zannini,L., Jekimovs,C. *et al.* (2006) Che-1 phosphorylation by ATM/ATR and Chk2 kinases activates p53 transcription and the G(2)/M checkpoint. *Cancer Cell*, **10**, 473–486.
20. Desantis,A., Bruno,T., Catena,V., De Nicola,F., Goeman,F., Iezzi,S., Sorino,C., Gentileschi,M.P., Germoni,S., Monteleone,V. *et al.* (2015) Che-1 modulates the decision between cell cycle arrest and apoptosis by its binding to p53. *Cell Death Dis.*, **6**, e1764.
21. Barbato,C., Corbi,N., Canu,N., Fanciulli,M., Serafino,A., Ciotti,M., Libri,V., Bruno,T., Amadoro,G., De Angelis,R. *et al.* (2003) Rb binding protein Che-1 interacts with Tau in cerebellar granule neurons. Modulation during neuronal apoptosis. *Mol. Cell Neurosci.*, **24**, 1038–1050.
22. Di Certo,M.G., Corbi,N., Bruno,T., Iezzi,S., De Nicola,F., Desantis,A, Mattei,E., Floridi,A., Fanciulli,M. *et al.* (2007) NRAGE associates with the anti-apoptotic factor Che-1 and regulates its degradation to induce cell death. *J. Cell Sci.*, **120**, 1852–1858.

23. Hopker,K., Hagmann,H., Khurshid,S., Chen,S., Hasskamp,P., Seeger-Nukpezah,T., Schilberg,K., Heukamp,L., Lamkemeyer,T., Sos,M.L. *et al.* (2012) AATF/Che-1 acts as a phosphorylation-dependent molecular modulator to repress p53-driven apoptosis. *EMBO J.*, **31**, 3961–3975.
24. Ferraris,S.E., Isoniemi,K., Torvaldson,E., Anckar,J., Westermarck,J. and Eriksson,J.E. (2012) Nucleolar AATF regulates c-Jun-mediated apoptosis. *Mol. Biol. Cell*, **23**, 4323–4332.
25. Tafforeau,L., Zorbas,C., Langhendries,J.L., Mullineux,S.T., Stamatopoulou,V., Mullier,R., Wacheul,L. and Lafontaine,D.L. (2013) The complexity of human ribosome biogenesis revealed by systematic nucleolar screening of Pre-rRNA processing factors. *Mol. Cell*, **51**, 539–551.
26. Badertscher,L., Wild,T., Montellese,C., Alexander,L.T., Bammert,L., Sarazova,M., Stebler,M., Csucs,G., Mayer,T.U., Zamboni,N. *et al.* (2015) Genome-wide RNAi screening identifies protein modules required for 40S subunit synthesis in human cells. *Cell Rep.*, **13**, 2879–2891.
27. Bammert,L., Jonas,S., Ungricht,R. and Kutay,U. (2016) Human AATF/Che-1 forms a nucleolar protein complex with NGDN and NOL10 required for 40S ribosomal subunit synthesis. *Nucleic Acids Res.*, **44**, 9803–9820.
28. Thomas,T., Voss,A.K., Petrou,P. and Gruss,P. (2000) The murine gene, Traube, is essential for the growth of preimplantation embryos. *Dev. Biol.*, **227**, 324–342.
29. Bruno,T., Desantis,A., Bossi,G., Di Agostino,S., Sorino,C., De Nicola,F., Iezzi,S., Franchitto,A., Benassi,B., Galanti,S. *et al.* (2010) Che-1 promotes tumor cell survival by sustaining mutant p53 transcription and inhibiting DNA damage response activation. *Cancer Cell*, **18**, 122–134.
30. Bruno,T., De Angelis,R., De Nicola,F., Barbato,C., Di Padova,M., Corbi,N., Libri,V., Benassi,B., Mattei,E., Chersi,A. *et al.* (2002) Che-1 affects cell growth by interfering with the recruitment of HDAC1 by Rb. *Cancer Cell*, **2**, 387–399.
31. De Nicola,F., Bruno,T., Iezzi,S., Di Padova,M., Floridi,A., Passananti,C., Del Sal,G. and Fanciulli,M. (2007) The prolyl isomerase Pin1 affects Che-1 stability in response to apoptotic DNA damage. *J. Biol. Chem.*, **282**, 19685–19691.
32. Andersen,J.S., Lam,Y.W., Leung,A.K., Ong,S.E., Lyon,C.E., Lamond,A.I. and Mann,M. (2005) Nucleolar proteome dynamics. *Nature*, **433**, 77–83.
33. Livak,K.J. and Schmittgen,T.D. (2001) Analysis of relative gene expression data using real-time quantitative PCR and the 2(-Delta Delta C(T)) Method. *Methods*, **25**, 402–408.
34. Schmidt,E.K., Clavarino,G., Ceppi,M. and Pierre,P. (2009) SUnSET, a nonradioactive method to monitor protein synthesis. *Nat. Methods*, **6**, 275–277.
35. Cox,J. and Mann,M. (2008) MaxQuant enables high peptide identification rates, individualized p.p.b.-range mass accuracies and proteome-wide protein quantification. *Nat. Biotechnol.*, **26**, 1367–1372.
36. Tusher,V.G., Tibshirani,R. and Chu,G. (2001) Significance analysis of microarrays applied to the ionizing radiation response. *Proc. Natl. Acad. Sci. U.S.A.*, **98**, 5116–5121.
37. Granneman,S. and Baserga,S.J. (2005) Crosstalk in gene expression: coupling and co-regulation of rDNA transcription, pre-ribosome assembly and pre-rRNA processing. *Curr. Opin. Cell Biol.*, **17**, 281–286.
38. Pineiro,D., Stoneley,M., Ramakrishna,M., Alexandrova,J., Dezi,V., Juke-Jones,R., Lilley,K.S., Cain,K. and Willis,A.E. (2018) Identification of the RNA polymerase I-RNA interactome. *Nucleic Acids Res.*, **46**, 11002–11013.
39. Kaiser,R.W.J., Ignarski,M., Van Nostrand,E.L., Frese,C.K., Jain,M., Cukoski,S., Heinen,H., Schaechter,M., Seufert,L., Bunte,K. *et al.* (2019) A protein-RNA interaction atlas of the ribosome biogenesis factor AATF. *Sci. Rep.*, **9**, 11071.
40. Craig,N., Kass,S. and Sollner-Webb,B. (1987) Nucleotide sequence determining the first cleavage site in the processing of mouse precursor rRNA. *Proc. Natl. Acad. Sci. U.S.A.*, **84**, 629–633.
41. Cui,C. and Tseng,H. (2004) Estimation of ribosomal RNA transcription rate in situ. *Biotechniques*, **36**, 134–138.
42. Ghoshal,K., Majumder,S., Datta,J., Motiwala,T., Bai,S., Sharma,S.M., Frankel,W. and Jacob,S.T. (2004) Role of human ribosomal RNA (rRNA) promoter methylation and of methyl-CpG-binding protein MBD2 in the suppression of rRNA gene expression. *J. Biol. Chem.*, **279**, 6783–6793.
43. Di Padova,M., Bruno,T., De Nicola,F., Iezzi,S., D'Angelo,C., Gallo,R., Nicosia,D., Corbi,N., Biroccio,A., Floridi,A. *et al.* (2003) Che-1 arrests human colon carcinoma cell proliferation by displacing HDAC1 from the p21WAF1/CIP1 promoter. *J. Biol. Chem.*, **278**, 36496–36504.
44. Ali,S.A., Dobson,J.R., Lian,J.B., Stein,J.L., van Wijnen,A.J., Zaidi,S.K. and Stein,G.S. (2012) A RUNX2-HDAC1 co-repressor complex regulates rRNA gene expression by modulating UBF acetylation. *J. Cell Sci.*, **125**, 2732–2739.
45. Hirschler-Laszkiewicz,I., Cavanaugh,A., Hu,Q., Catania,J., Avantaggiati,M.L. and Rothblum,L.I. (2001) The role of acetylation in rDNA transcription. *Nucleic Acids Res.*, **29**, 4114–4124.
46. Cong,R., Das,S., Ugrinova,I., Kumar,S., Mongelard,F., Wong,J. and Bouvet,P. (2012) Interaction of nucleolin with ribosomal RNA genes and its role in RNA polymerase I transcription. *Nucleic Acids Res.*, **40**, 9441–9454.
47. van Sluis,M. and McStay,B. (2017) Nucleolar reorganization in response to rDNA damage. *Curr. Opin. Cell Biol.*, **46**, 81–86.
48. Shav-Tal,Y., Blechman,J., Darzacq,X., Montagna,C., Dye,B.T., Patton,J.G., Singer,R.H. and Zipori,D. (2005) Dynamic sorting of nuclear components into distinct nucleolar caps during transcriptional inhibition. *Mol. Biol. Cell*, **16**, 2395–2413.
49. Perry,R.P. and Kelley,D.E. (1968) Persistent synthesis of 5S RNA when production of 28S and 18S ribosomal RNA is inhibited by low doses of actinomycin D. *J. Cell Physiol.*, **72**, 235–246.
50. Drygin,D., Lin,A., Bliesath,J., Ho,C.B., O'Brien,S.E., Proffitt,C., Omori,M., Haddach,M., Schwaebe,M.K., Siddiqui-Jain,A. *et al.* (2011) Targeting RNA polymerase I with an oral small molecule CX-5461 inhibits ribosomal RNA synthesis and solid tumor growth. *Cancer Res.*, **71**, 1418–1430.
51. Burger,K., Muhl,B., Harasim,T., Rohrmoser,M., Malamoussi,A., Orban,M., Kellner,M., Gruber-Eber,A., Kremmer,E., Holzel,M. *et al.* (2010) Chemotherapeutic drugs inhibit ribosome biogenesis at various levels. *J. Biol. Chem.*, **285**, 12416–12425.
52. Sun,X.X., Dai,M.S. and Lu,H. (2008) Mycophenolic acid activation of p53 requires ribosomal proteins L5 and L11. *J. Biol. Chem.*, **283**, 12387–12392.
53. Mahajan,P.B. and Thompson,E.A. Jr (1987) Cyclosporin A inhibits rDNA transcription in lymphosarcoma P1798 cells. *J. Biol. Chem.*, **262**, 16150–16156.
54. Emmott,E. and Hiscox,J.A. (2009) Nucleolar targeting: the hub of the matter. *EMBO Rep.*, **10**, 231–238.
55. Grob,A. and McStay,B. (2014) Construction of synthetic nucleoli and what it tells us about propagation of sub-nuclear domains through cell division. *Cell Cycle*, **13**, 2501–2508.
56. Farley,K.I., Surovtseva,Y., Merkel,J. and Baserga,S.J. (2015) Determinants of mammalian nucleolar architecture. *Chromosoma*, **124**, 323–331.
57. Ugrinova,I., Monier,K., Ivaldi,C., Thiry,M., Storck,S., Mongelard,F. and Bouvet,P. (2007) Inactivation of nucleolin leads to nucleolar disruption, cell cycle arrest and defects in centrosome duplication. *BMC Mol. Biol.*, **8**, 66.
58. Hamdane,N., Stefanovsky,V.Y., Tremblay,M.G., Nemeth,A., Paquet,E., Lessard,F., Sanij,E., Hannan,R. and Moss,T. (2014) Conditional inactivation of Upstream Binding Factor reveals its epigenetic functions and the existence of a somatic nucleolar precursor body. *PLoS Genet.*, **10**, e1004505.
59. Farley-Barnes,K.I., McCann,K.L., Ogawa,L.M., Merkel,J., Surovtseva,Y.V. and Baserga,S.J. (2018) Diverse regulators of human ribosome biogenesis discovered by changes in nucleolar number. *Cell Rep.*, **22**, 1923–1934.
60. Kruhlak,M., Crouch,E.E., Orlov,M., Montano,C., Gorski,S.A., Nussenzweig,A., Misteli,T., Phair,R.D. and Casellas,R. (2007) The ATM repair pathway inhibits RNA polymerase I transcription in response to chromosome breaks. *Nature*, **447**, 730–734.
61. Velichko,A.K., Petrova,N.V., Luzhin,A.V., Strelkova,O.S., Ovsyannikova,N., Kireev,II, Petrova,N.V., Razin,S.V. and Kantidze,O.L. (2019) Hypoosmotic stress induces R loop formation in nucleoli and ATR/ATM-dependent silencing of nucleolar transcription. *Nucleic Acids Res.*, **47**, 6811–6825.
62. Pati,U.K. (1994) Human RNA polymerase II subunit hRPB14 is homologous to yeast RNA polymerase I, II, and III subunits (AC19

and RPB11) and is similar to a portion of the bacterial RNA polymerase alpha subunit. *Gene*, **145**, 289–292.
63. Jacob,M.D., Audas,T.E., Mullineux,S.T. and Lee,S. (2012) Where no RNA polymerase has gone before: novel functional transcripts derived from the ribosomal intergenic spacer. *Nucleus*, **3**, 315–319.
64. Zencir,S., Sike,A., Dobson,M.J., Ayaydin,F., Boros,I. and Topcu,Z. (2013) Identification of transcriptional and phosphatase regulators as interaction partners of human ADA3, a component of histone acetyltransferase complexes. *Biochem. J.*, **450**, 311–320.
65. Gallagher,J.E., Dunbar,D.A., Granneman,S., Mitchell,B.M., Osheim,Y., Beyer,A.L. and Baserga,S.J. (2004) RNA polymerase I transcription and pre-rRNA processing are linked by specific SSU processome components. *Genes Dev.*, **18**, 2506–2517.
66. Kong,R., Zhang,L., Hu,L., Peng,Q., Han,W., Du,X. and Ke,Y. (2011) hALP, a novel transcriptional U three protein (t-UTP), activates RNA polymerase I transcription by binding and acetylating the upstream binding factor (UBF). *J. Biol. Chem.*, **286**, 7139–7148.
67. Tsai,Y.C., Greco,T.M., Boonmee,A., Miteva,Y. and Cristea,I.M. (2012) Functional proteomics establishes the interaction of SIRT7 with chromatin remodeling complexes and expands its role in regulation of RNA polymerase I transcription. *Mol. Cell Proteomics*, **11**, 60–76.
68. Ford,E., Voit,R., Liszt,G., Magin,C., Grummt,I. and Guarente,L. (2006) Mammalian Sir2 homolog SIRT7 is an activator of RNA polymerase I transcription. *Genes Dev.*, **20**, 1075–1080.
69. Grandori,C., Gomez-Roman,N., Felton-Edkins,Z.A., Ngouenet,C., Galloway,D.A., Eisenman,R.N. and White,R.J. (2005) c-Myc binds to human ribosomal DNA and stimulates transcription of rRNA genes by RNA polymerase I. *Nat. Cell Biol.*, **7**, 311–318.
70. van Riggelen,J., Yetil,A. and Felsher,D.W. (2010) MYC as a regulator of ribosome biogenesis and protein synthesis. *Nat. Rev. Cancer*, **10**, 301–309.
71. Geuskens,M. and Alexandre,H. (1984) Ultrastructural and autoradiographic studies of nucleolar development and rDNA transcription in preimplantation mouse embryos. *Cell Differ.*, **14**, 125–134.
72. Bywater,M.J., Pearson,R.B., McArthur,G.A. and Hannan,R.D. (2013) Dysregulation of the basal RNA polymerase transcription apparatus in cancer. *Nat. Rev. Cancer*, **13**, 299–314.
73. Pelletier,J., Thomas,G. and Volarevic,S. (2018) Ribosome biogenesis in cancer: new players and therapeutic avenues. *Nat. Rev. Cancer*, **18**, 51–63.
74. Bustelo,X.R. and Dosil,M. (2018) Ribosome biogenesis and cancer: basic and translational challenges. *Curr. Opin. Genet. Dev.*, **48**, 22–29.
75. Perez-Riverol,Y., Csordas,A., Bai,J.W., Bernal-Llinares,M., Hewapathirana,S., Kundu,D.J., Inuganti,A., Griss,J., Mayer,G., Eisenacher,M. *et al.* (2019) The PRIDE database and related tools and resources in 2019: improving support for quantification data. *Nucleic Acids Res.*, **47**, D442–D450.